JOURNAL OF GUIDANCE, CONTROL, AND DYNAMICS
Vol. 43, No. 3, March 2020

Multiple-Timescale Nonlinear Control of Aircraft with Model Uncertainties

Dipanjan Saha,* John Valasek,† Christopher Leshikar,‡ and Mohammad M. Reza‡
Texas A&M University, College Station, Texas 77843-3141

https://doi.org/10.2514/1.G004303

This paper develops a multiple-timescale slow state tracking nonlinear controller to accomplish large-amplitude combined longitudinal and lateral/directional maneuvers of a nonlinear, nonstandard six-degree-of-freedom aircraft model in the presence of uncertain inertias, control derivatives, and an engine time constant. The control synthesis uses the evolution of the slow states, slow actuators, fast states and fast actuators in a total of four different timescales. Multiplicative and additive uncertainties in the evolution of the slow and the fast states are accounted for, as well as multiplicative uncertainties in the slow and fast actuator dynamics. The controller is designed with insights from geometric singular perturbation theory, and it is supported by update laws selected via a composite Lyapunov analysis. The boundedness of the tracking errors, manifold errors and parameter estimation errors is proven; and the magnitudes of the tracking errors, parameter estimation errors, and control signals can be modulated by appropriate choices of gains. The results presented in the paper using a nonlinear six-degree-of-freedom simulation show improved velocity control for the multiple-timescale nonlinear controller as compared to a cascaded nonlinear dynamic inversion controller.

Nomenclature

B_X, B_{XY}	=	constant but unknown parameter matrices in the dynamics
$b_{XY_{ij}}$	=	the (i, j)th element of matrix B_{XY}
f_X, F_{XY}	=	vector and matrix functions representing how states evolve on their own
f_{X_i}	=	the ith element of a vector function f_X
G_{XY}	=	matrix functions representing how actuators (commands) dictate the evolution of states (actuators)
$\hat{p}$	=	estimate of an unknown parameter p
$\|Q\|_2$	=	the induced 2-norm of a matrix Q; equivalently, its largest singular value
$\mathbb{R}$	=	the space of real numbers
$\mathbb{R}^n$	=	the n-dimensional real space
u_f	=	fast control
u_s	=	slow control
X, Y	=	generic subscripts
x	=	kinetic slow states
$\dot{x}$	=	derivative of x with respect to the slowest timescale
$\grave{x}$	=	derivative of x with respect to the second slowest timescale
x'	=	derivative of x with respect to the second fastest timescale
$\breve{x}$	=	derivative of x with respect to the fastest timescale
z	=	fast states
α_i	=	weights of individual Lyapunov functions in the composite Lyapunov function
δ_f	=	fast actuators
δ_s	=	slow actuators
ε	=	timescale parameter for fast states
θ_i	=	gains used in the parameter update laws
Λ_{XY}	=	constant but unknown parameter matrices in control distribution
$\lambda_{\min}(A)$	=	minimum eigenvalue of a matrix A
$\lambda_{XY_{ij}}$	=	the (i, j)th element of a matrix Λ_{XY}
$\|v\|_2$	=	the 2-norm (Euclidean norm) of a vector v
$\|v\|_\infty$	=	the infinity norm of a vector v
ξ	=	kinematic slow states
ρ	=	timescale parameter for fast actuators
σ	=	timescale parameter for slow actuators

Received 31 December 2018; revision received 29 September 2019; accepted for publication 30 September 2019; published online 18 December 2019.

*Research Assistant, Vehicle Systems and Control Laboratory, Department of Aerospace Engineering. Member AIAA.

†Professor and Director, Vehicle Systems and Control Laboratory, Department of Aerospace Engineering. Fellow AIAA.

‡Undergraduate Research Assistant, Vehicle Systems and Control Laboratory, Department of Aerospace Engineering. Student Member AIAA.

I. Introduction

DYNAMICS evolving in distinct slow and fast timescales are observed in systems such as aircraft [1], spacecraft [2], robotic manipulators [3], electrical power systems [4], biochemical reactions [5], nuclear reactors [6], production planning in manufacturing [7], etc. The geometric singular perturbation theory [8,9] is a powerful control law development tool for multiple-timescale systems because it provides physical insight into the evolution of the states in more than one timescales. Controller design using the geometric singular perturbation (GSP) approach offers three benefits [10]. First, it does not require linearization of the plant in order to synthesize a controller. Second, the controller so designed does not use gain scheduling to address the space of operating conditions. Third, the use of lower-order reduced subsystems makes the design of controllers for high-dimensional systems less complex and less susceptible to the "curse of dimensionality" [11]. Even though the approach uses lower-order subsystems, the composite Lyapunov analysis [12] establishes the bounds of timescale separation within which the stability of the full-order nonlinear system is guaranteed. In the context of flight control design, the GSP approach retains the coupling between the slow and the fast dynamics in different timescales (e.g., phugoid and short period modes) rather than representing the plant as decoupled phugoid and short-period approximations, for instance.

A generic nonlinear system with two timescales can be represented as

$$\dot{x} = f(x, z, u)$$
$$\varepsilon \dot{z} = g(x, z, u) \tag{1}$$

where x is the slow state, z is the fast state, u is the control input, $f(.), g(.)$ are nonlinear functions, and ε is the timescale separation parameter satisfying $0 < \varepsilon \ll 1$. Two extreme cases of timescale separation are $\varepsilon = 0$, which represents infinite separation (i.e., the fast dynamics are infinitely fast), and $\varepsilon = 1$, which represents no separation (i.e., the rates of evolution of states x and z are similar). According to GSP theory, the slow timescale is one in which the slow state x

evolves and the fast state z stays on some equilibrium manifold z^0. The fast timescale is one in which the slow state x remains "frozen" at its initial condition and the fast state z evolves to its equilibrium manifold z^0. To define the manifold mathematically, substitute $\varepsilon = 0$ in Eq. (1) to obtain

$$\dot{x} = f(x, z^0, u)$$
$$0 = g(x, z^0, u) \tag{2}$$

The manifold $z^0(x, u)$ is an isolated real root of the algebraic equation $g(x, z^0, u) = 0$. If it is possible to compute a manifold $z^0(x, u)$ that is an exact solution of $g(x, z^0, u) = 0$, system (1) is called a standard system. Otherwise, it is called a nonstandard system. If the function $g(.)$ is nonlinear in the fast state z, the system is in general nonstandard. The fast states for an aircraft are typically the body-axis angular rates. The angular accelerations are nonlinear in the rates, thus aircraft are examples of nonstandard systems. Although many works in the literature addressed standard systems [13–21], the theory of control design for nonstandard systems (specifically, nonlinear, nonstandard systems) were explored only recently [10,22]. One of the important control objectives for nonstandard systems is slow state tracking. For this objective, the fast states are allowed to settle onto any suitable equilibrium manifold. The method of modified composite control approximates the manifold [22], whereas the method of sequential control specifies the manifold [10] as an intermediate control variable. The fundamental idea behind sequential control is to use feedback to convert an open-loop nonstandard system into a closed-loop standard system.

Earlier work on two-timescale aircraft flight control can be found in papers by Khalil and Chen [1] and Menon et al. [23]. A nonlinear six-degree-of-freedom (6-DOF) aircraft is an interesting example of a multiple-timescale system because aircraft have slow and fast states as well as slow and fast actuators. Velocity, aerodynamic angles, and kinematic angles are the slow states; body-axis roll, and pitch and yaw rates are the fast states. Because of the slow engine dynamics, the throttle is considered a slow actuator, whereas aerodynamic control surfaces are considered fast actuators. Some recent works applied the theory of slow state tracking for nonstandard multiple-timescale systems to solve aircraft flight control problems. Modified composite control was applied to a nonlinear 6-DOF generic F/A-18A commanded to perform a 45 deg turn [24]. The angle of attack, sideslip angle, and heading angle were the states to be tracked. All of the aerodynamic controls were assumed infinitely fast. The engine dynamics were not accounted for, and the throttle was held constant throughout the maneuver. As a result, the Mach number decreased from 0.3 to below 0.2 and never recovered as the aircraft turned. Although it was not straightforward to include actuator dynamics in the modified composite control, the method of sequential control was extended to account for slow and fast actuator dynamics in the control synthesis [10]. In a previous work by Saha et al., this method was applied to a nonlinear 6-DOF generic F-16A commanded to perform two large-amplitude combined longitudinal and lateral/directional maneuvers [25]. One of the evaluation maneuvers was motivated by the modified torsional agility parameter, which is a constant-altitude 90 deg banked turn followed by a rapid roll reversal to an opposite 90 deg banked turn [26]. The second evaluation maneuver was a turn sequence for which the pilot inputs were generated by flying a generic F-16A in a cockpit-based nonlinear 6-DOF flight simulator. The loss of airspeed during turns was significantly reduced for both of the maneuvers. In particular, the loss of airspeed for a 90 deg turn was within 50 ft/s and the velocity rapidly returned to the trim value upon completion of the turn. A major limitation of the method of sequential control applied to aircraft maneuvers is the assumption of a deterministic model. A nonlinear 6-DOF aircraft model has several sources of uncertainty. Accurate numerical values of inertias can be obtained by using other methods. However, those methods cost a lot of time and money. The class-I methods are meant for quick estimates at zero financial cost, even though the inertia estimates may be "rough" estimates [27]. The aerodynamics are often modeled using stability and control derivatives, with the control derivatives being more difficult to estimate accurately than the stability derivatives. The engine is often the slowest primary control actuator in the system for which the turbomachinery can be modeled as a linear first-order system but with a time constant that is not always known exactly. The uncertainties in inertias, control derivatives, and engine time constants are parametric or multiplicative uncertainties. The errors between the actual and modeled aerodynamics can be viewed as additive uncertainties because the aerodynamic forces and moments can be modeled as first-order Taylor series approximations, with the first-order partial derivatives being the stability and control derivatives.

Some of the authors' previous works developed controllers for uncertain nonlinear, nonstandard multiple-timescale systems. However, the scope of these works does not cover the class of systems of which aircraft are examples. A slow state regulator for an uncertain nonlinear nonstandard two-timescale system was developed in the work of Saha et al. [28]. This work considered multiplicative and additive uncertainties in the fast dynamics. The controller used the estimate of the unknown parameter and the worst-case equivalent of the additive uncertainty. An online parameter estimator updated the parameter estimate, and the update law was selected from the composite Lyapunov analysis. This analysis, followed by an application of Barbalat's lemma [29], proved the convergence of the fast state to its equilibrium manifold and the slow state to zero. The stability analysis also showed that the parameter estimation error remains bounded but does not necessarily converge to zero. This work did not consider actuator dynamics. A recent work of Saha and Valasek [30] developed a three-timescale attitude tracking controller for a nonlinear, nonstandard spacecraft with uncertain inertias. This work considered a separate timescale of the actuators in addition to the timescales of the slow and the fast states. In addition, it considered parametric uncertainties in the dynamics and in the control distribution of the fast states only. The slow states represented the kinematics, and they did not have any uncertainty in their evolution. The actuator dynamics were not modeled with any uncertainty.

Developing a slow state tracking controller for an aircraft with model uncertainties is challenging for several reasons. In contrast to the spacecraft attitude tracking problem where the controller influences rotational motion only, an aircraft flight controller must influence both translational and rotational motions (i.e., both velocity and attitude) at the same time. To consider velocity and attitude dynamics together, the actuators must be discriminated as slow and fast. For spacecraft attitude tracking, the uncertainties are in the fast dynamics, i.e., the angular rates only. Aircraft, by comparison, have uncertainties in the dynamics of the kinetic slow states and the fast states, as well as the actuators. Reference [25] showed the deterministic version of a Lyapunov-based four-timescale GSP flight controller, but no previous result is available to show how uncertainties can be handled in a way that guarantees the stability of the full-order system for the case with actuators classified as slow and fast. Moreover, the GSP approach has not yet been compared with one of the standard flight control design methodologies to ascertain whether accounting for timescales in the system produces a more effective controller. This paper makes two contributions in multiple-timescale nonlinear control of nonlinear 6-DOF aircraft. First, a four-timescale slow state tracking nonlinear controller is developed using the GSP approach and a Lyapunov-based online parameter estimator. The controller is designed to handle multiplicative and additive uncertainties in the model and keep all of the errors ultimately bounded. Second, the multiple-timescale nonlinear controller using the GSP approach is directly compared to the well-known cascaded nonlinear dynamic inversion (NDI) controller [31,32]. The aircraft is commanded to perform a combined longitudinal and lateral/directional evaluation maneuver, consisting of a steep climb to reduce velocity, followed by back-to-back turns. This maneuver is used to compare the Euler angle and velocity tracking performance of the two controllers.

The paper is organized as follows. Section II discusses the class of four-timescale systems and the control objective. Section III shows the control law development. Numerical results including the comparison of the GSP and the NDI approaches are in Sec. IV, and conclusions are in Sec. V.

II. Class of Systems and Control Objective

The principles of GSP are used to develop a slow state tracking controller for a class of nonlinear systems with multiple timescales, as well as multiplicative and additive uncertainties. The development

considers a total of four timescales: the slow states evolving in the slowest timescale; the slow actuators evolving in the second slowest timescale; the fast states evolving in the second fastest timescale; and the fast actuators evolving in the fastest timescale. The slow states to track are classified as kinetic and kinematic states. The kinetic slow states can be influenced directly by both the slow and the fast actuators. The kinematic slow states can be influenced directly by the fast states. The fast states can be influenced directly by the fast actuators but not by the slow actuators. Except for the kinematic slow states, all of the states and actuators have parametric uncertainties in their evolution. Moreover, time-dependent and state-dependent static uncertainties are considered as additive uncertainties in the evolution of the kinetic slow and the fast states. The controller is developed on the nonlinear state-space model:

$$\begin{aligned}
\dot{x} &= B_{xx} f_{xx}(x,\xi) + B_{xz} F_{xz}(x,\xi) z + \gamma_x(t,x,\xi,z) + \Lambda_{x\delta_s} G_{x\delta_s}(x,\xi)\delta_s \\
&\quad + \Lambda_{x\delta_f} G_{x\delta_f}(x,\xi)\delta_f \\
\dot{\xi} &= F_{\xi z}(x,\xi) z \\
\sigma\dot{\delta}_s &= B_{\delta_s} f_{\delta_s}(\delta_s) + \Lambda_{\delta_s u_s} G_{\delta_s u_s}(\delta_s) u_s \\
\varepsilon\dot{z} &= \sum_k B_z^k f_z^k(x,\xi,z) + \gamma_z(t,x,\xi,z) + \Lambda_{z\delta_f} G_{z\delta_f}(x,\xi)\delta_f \rho \\
\dot{\delta}_f &= B_{\delta_f} f_{\delta_f}(\delta_f) + \Lambda_{\delta_f u_f} G_{\delta_f u_f}(\delta_f) u_f
\end{aligned} \tag{3}$$

The conversion of nonlinear aircraft equations to the form in Eq. (3) and the mathematical expressions of the functions and matrices are provided in Appendix A. In Eq. (3), $x \in \mathbb{R}^n$ is the vector of n kinetic slow states, $\xi \in \mathbb{R}^m$ is the vector of m kinematic slow states, $z \in \mathbb{R}^m$ is the vector of m fast states, $\delta_s \in \mathbb{R}^n$ is the vector of n slow actuators, $\delta_f \in \mathbb{R}^m$ is the vector of m fast actuators, $u_s \in \mathbb{R}^n$ is the vector of n slow controls, and $u_f \in \mathbb{R}^m$ is the vector of m fast controls. In the context of an aircraft, $x = v_A$ is the velocity; $\xi = [\,\phi \quad \theta \quad \psi\,]^T$ are the three Euler angles; $z = [\,p \quad q \quad r\,]^T$ are the three body-axis angular rates; $\delta_s = \delta_t$ is the throttle; $\delta_f = [\,\delta_e \quad \delta_a \quad \delta_r\,]^T$ are the three aerodynamic control surfaces (elevator, aileron and rudder); $u_s = \delta_{t_c}$ is the throttle command; and $u_f = [\,\delta_{e_c} \quad \delta_{a_c} \quad \delta_{r_c}\,]$ are the commanded elevator, aileron, and rudder.

The "dot" represents the time derivative with respect to the slowest timescale t. The perturbation parameters σ, ε, and ρ satisfy $0 < \rho \ll \varepsilon \ll \sigma \ll 1$. The inclusion of three perturbation parameters leads to a total of three additional timescales. The second slowest timescale is $t_\sigma = (t/\sigma)$; the second fastest timescale is $t_\varepsilon = (t/\varepsilon)$, and the fastest timescale is $t_\rho = (t/\rho)$. These timescale parameters are added artificially to the aircraft dynamics to show explicitly which states evolve in which timescale.

The multiplicative uncertainties are captured in the constant but unknown matrices B_{xx}, B_{xz}, $\Lambda_{x\delta_s}$, $\Lambda_{x\delta_f}$, B_{δ_s}, $\Lambda_{\delta_s u_s}$, B_z^k, $\Lambda_{z\delta_f}$, B_{δ_f}, and $\Lambda_{\delta_f u_f}$. It is assumed that every unknown parameter p_{ij} in each parameter matrix is bounded between a known lower bound $\underline{p}_{ij}$ and a known upper bound $\bar{p}_{ij}$, i.e., $p_{ij} \in [\underline{p}_{ij}, \bar{p}_{ij}]$. The additive uncertainties are included in the unknown vectors of functions $\gamma_x(.)$ and $\gamma_z(.)$. Even though the exact forms of these functions are unknown, it is assumed that the Euclidean norms satisfy

$$\|\gamma_x(t,x,\xi,z)\|_2 \le \kappa_1\|x\|_2 + \kappa_2\|\xi\|_2 + \kappa_3\|z\|_2$$

and

$$\|\gamma_z(t,x,\xi,z)\|_2 \le \kappa_4\|x\|_2 + \kappa_5\|\xi\|_2 + \kappa_6\|z\|_2$$

for some known constants $\kappa_i \ge 0$; $i = 1,\ldots,6$. For the aircraft problem, the multiplicative uncertainties represent inertias, aerodynamic derivatives, and actuator characteristics; whereas the additive uncertainties represent modeling errors, such as using a first-order Taylor series approximation to model the aerodynamics. It is assumed that the induced 2-norms or, equivalently, the largest singular values of the matrices satisfy the following: $\bar{\sigma}(B_{xz}) \le v_1$, $\bar{\sigma}(F_{xz}) \le v_2$, $\bar{\sigma}(\Lambda_{x\delta_s}) \le v_3$, $\bar{\sigma}(G_{x\delta_s}) \le v_4$, $\bar{\sigma}(\Lambda_{x\delta_f}) \le v_5$, $\bar{\sigma}(G_{x\delta_s}) \le v_6$, $\bar{\sigma}(F_{\xi z}) \le v_7$, $\bar{\sigma}(\Lambda_{z\delta_f}) \le v_8$, and $\bar{\sigma}(G_{z\delta_f}) \le v_9$ for some known constants v_i; $i = 1,\ldots,9$. The vectors and matrices of functions are assumed to consist of known smooth functions. The matrices $G_{x\delta_s}$, $F_{\xi z}$, $G_{\delta_s u_s}$, $G_{z\delta_f}$, and $G_{\delta_f u_f}$ are assumed to be full rank.

The control objective is to design the slow control vector u_s and the fast control vector u_f such that the kinetic slow state vector $x(t)$ tracks a twice differentiable reference trajectory $x_r(t)$, and the kinematic slow state vector $\xi(t)$ tracks a twice differentiable reference trajectory $\xi_r(t)$. To achieve this objective using the GSP approach, the fast states z need to be stabilized on a suitable equilibrium manifold z^0, the slow actuators δ_s need to be stabilized on a suitable equilibrium manifold δ_s^0, and the fast actuators need to be stabilized on a suitable equilibrium manifold δ_f^0. It is to be noted that the fast states, the slow actuators, and the fast actuators work as intermediate control variables that are designed in different timescales. Define the tracking errors $e_x := x - x_r$ and $e_\xi := \xi - \xi_r$ and the manifold errors $e_z := z - z^0$, $e_{\delta_s} := \delta_s - \delta_s^0$, and $e_{\delta_f} := \delta_f - \delta_f^0$. The tracking problem now becomes an equivalent stabilization problem for the error system:

$$\begin{aligned}
\dot{e}_x &= B_{xx} f_{xx}(.) + B_{xz} F_{xz}(.)(e_z + z^0) + \gamma_x(.) + \Lambda_{x\delta_s} G_{x\delta_s}(.)(e_{\delta_s} + \delta_s^0) \\
&\quad + \Lambda_{x\delta_f} G_{x\delta_f}(.)(e_{\delta_f} + \delta_f^0) - \dot{x}_r \\
\dot{e}_\xi &= F_{\xi z}(.)(e_z + z^0) - \dot{\xi}_r \\
\sigma\dot{e}_{\delta_s} &= B_{\delta_s} f_{\delta_s}(.) + \Lambda_{\delta_s u_s} G_{\delta_s u_s}(.) u_s - \sigma\dot{\delta}_s^0 \\
\varepsilon\dot{e}_z &= \sum_k B_z^k f_z^k(.) + \gamma_z(.) + \Lambda_{z\delta_f} G_{z\delta_f}(.)(e_{\delta_f} + \delta_f^0) - \varepsilon\dot{z}^0 \\
\rho\dot{e}_{\delta_f} &= B_{\delta_f} f_{\delta_f}(.) + \Lambda_{\delta_f u_f} G_{\delta_f u_f}(.) u_f - \rho\dot{\delta}_f^0
\end{aligned} \tag{4}$$

The arguments of the functions f_{xx}, F_{xz}, etc., are the same as those in Eq. (3). Henceforth, the arguments will not be shown explicitly unless they are different from those in Eq. (3).

III. Control Law Development

The control law development involves two major stages. The first stage is the design of a sequential timescale controller using principles of GSP with estimates of the constant but unknown parameter matrices. Using lower-order reduced subsystems, different parts of the controller are designed in such a way that stability of each subsystem in the sense of Lyapunov is guaranteed when the parameter estimates are perfect. The second stage in the development is the design of the update laws for the constant but unknown parameters such that stability in the sense of Lyapunov is ensured for the full-order system.

A. Design of the Four-Timescale Sequential Controller

A schematic of the controller design in four timescales is shown in Fig. 1. The numbers 1, 2, 3, and 4 on the schematic indicate the sequence in which the specific design variables appear in the control law development.

1. Design of Manifold of Fast States and Slow Actuators in Slowest Timescale

In the slowest timescale t, it is assumed that the fast states are on the manifold z^0, the slow actuators are on the manifold δ_s^0, and the fast actuators are on a special case of the manifold $\delta_f^0|_{z^0}$. The manifolds z^0 and δ_s^0 are selected such that the slow state error vectors e_x and e_ξ go to zero. To construct the reduced subsystem, the constant but unknown parameter matrices B_{xx}, B_{xz}, $\Lambda_{x\delta_s}$, and $\Lambda_{x\delta_f}$ are replaced by their estimates $\hat{B}_{xx}$, $\hat{B}_{xz}$, $\hat{\Lambda}_{x\delta_s}$, and $\hat{\Lambda}_{x\delta_f}$, respectively; and the additive uncertainty γ_x is ignored. The reduced subsystem in the slowest timescale is

$$\begin{aligned}
\dot{e}_x &= \hat{B}_{xx} f_{xx} + \hat{B}_{xz} F_{xz} z^0 - \dot{x}_r + \hat{\Lambda}_{x\delta_s} G_{x\delta_s} \delta_s^0 + \hat{\Lambda}_{x\delta_f} G_{x\delta_f} \delta_f^0|_{z^0} \\
\dot{e}_\xi &= F_{\xi z} z^0 - \dot{\xi}_r
\end{aligned} \tag{5}$$

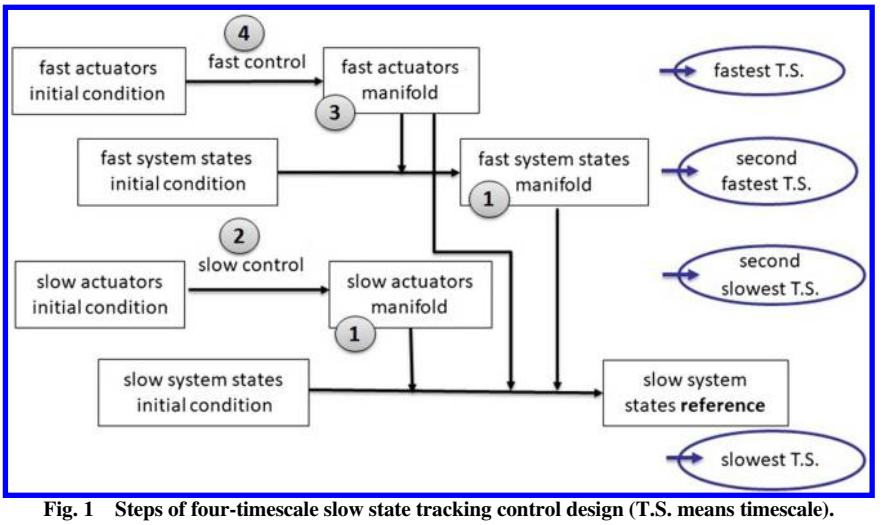

Fig. 1 Steps of four-timescale slow state tracking control design (T.S. means timescale).

A positive-definite candidate Lyapunov function for subsystem (5) is selected as

$$V_1 = \frac{1}{2}e_x^T e_x + \frac{1}{2}e_\xi^T e_\xi \tag{6}$$

Along the trajectories of subsystem (5), the time derivative of the Lyapunov function V_1 is

$$\dot{V}_1|_{(5)} = e_x^T(\hat{B}_{xx}f_{xx} + \hat{B}_{xz}F_{xz}z^0 + \hat{\Lambda}_{x\delta_s}G_{x\delta_s}\delta_s^0 + \hat{\Lambda}_{x\delta_f}G_{x\delta_f}\delta_f^0|_{z^0} - \dot{x}_r) + e_\xi^T(F_{\xi z}z^0 - \dot{\xi}_r) \tag{7}$$

where $f|_{(i)}$ denotes the value of the function $f(.)$ for a system represented by a generic equation (i). Suppose that the manifold of the fast states z^0 is selected as

$$z^0 = F_{\xi z}^{-1}(\dot{\xi}_r - K_\xi e_\xi) \tag{8}$$

and that the manifold of the slow actuators δ_s^0 is selected as

$$\delta_s^0 = G_{x\delta_s}^{-1}\hat{\Lambda}_{x_{\delta_s}}^{-1}(\dot{x}_r - \hat{B}_{xx}f_{xx} - \hat{B}_{xz}F_{xz}z^0 - \hat{\Lambda}_{x\delta_f}G_{x\delta_f}\delta_f^0|_{z^0} - K_x e_x) \tag{9}$$

where $\hat{\Lambda}_{x_{\delta_s}}$ is assumed full rank, and $\delta_f^0|_{z^0}$ is yet to be determined. For these choices, the time derivative of the Lyapunov function V_1 for reduced subsystem (5) becomes

$$\dot{V}_1|_{(5)} = -e_x^T K_x e_x - e_\xi^T K_\xi e_\xi \tag{10}$$

This is negative definite for any positive-definite K_x and K_ξ, indicating that the equilibrium $e_x = 0$ and $e_\xi = 0$ of reduced subsystem (5) is stable in the sense of Lyapunov. Note that the use of kinetic and kinematic slow states enables sequential selections of the manifolds z^0 and δ_s^0 in the control design.

2. Design of Slow Control in Second Slowest Timescale

In the second slowest timescale $t_\sigma = (t/\sigma)$, the slow controls u_s are designed such that the slow actuators δ_s reach their manifold δ_s^0; consequently, slow actuator errors e_{δ_s} go to zero. The reduced subsystem in the second slowest timescale is

$$\grave{e}_{\delta_s} = \hat{B}_{\delta_s}f_{\delta_s} + \hat{\Lambda}_{\delta_s u_s}G_{\delta_s u_s}u_s \tag{11}$$

which uses the estimates of the unknown parameter matrices B_{δ_s} and $\Lambda_{\delta_s u_s}$. A positive-definite candidate Lyapunov function for this subsystem is selected as

$$V_2 = \frac{1}{2}e_{\delta_s}^T e_{\delta_s} \tag{12}$$

Along the trajectories of reduced subsystem (11), the time derivative of V_2 is

$$\grave{V}_2|_{(11)} = e_{\delta_s}^T(\hat{B}_{\delta_s}f_{\delta_s} + \hat{\Lambda}_{\delta_s u_s}G_{\delta_s u_s}u_s) \tag{13}$$

If the vector of slow controls u_s is selected as

$$u_s = G_{\delta_s u_s}^{-1}\hat{\Lambda}_{\delta_s u_s}^{-1}(-\hat{B}_{\delta_s}f_{\delta_s} - K_{\delta_s}e_{\delta_s}) \tag{14}$$

then the derivative of the Lyapunov function V_2 with respect to the second slowest timescale becomes

$$\grave{V}_2|_{(11)} = -e_{\delta_s}^T K_{\delta_s}e_{\delta_s} \tag{15}$$

which is negative definite for any positive-definite K_{δ_s}. Thus, the equilibrium $e_{\delta_s} = 0$ of reduced subsystem (11) is stable in the sense of Lyapunov.

3. Design of Manifold of Fast Actuators in Second Fastest Timescale

In the second fastest timescale $t_\varepsilon = (t/\varepsilon)$, the manifold of the fast actuators δ_f^0 is selected such that the fast states z reach their manifold z^0 or, equivalently, the fast state error vector e_z becomes zero. To construct the reduced subsystem, the constant but unknown parameter matrices B_z^k and $\Lambda_{z\delta_f}$ are replaced by their estimates $\hat{B}_z^k$ and $\hat{\Lambda}_{z\delta_f}$, respectively, and the additive uncertainty γ_z is ignored. The reduced subsystem in the second fastest timescale is

$$e_z' = \sum_k \hat{B}_z^k f_z^k + \hat{\Lambda}_{z\delta_f}G_{z\delta_f}\delta_f^0 \tag{16}$$

A positive-definite candidate Lyapunov function for this subsystem is

$$V_3 = \frac{1}{2}e_z^T e_z \tag{17}$$

Along the trajectories of subsystem (16), the time derivative of this Lyapunov function is

$$V_3'|_{(16)} = e_z^T\left(\sum_k \hat{B}_z^k f_z^k + \hat{\Lambda}_{z\delta_f}G_{z\delta_f}\delta_f^0\right) \tag{18}$$

If the manifold of the fast actuators is selected as

$$\delta_f^0 = G_{z\delta_f}^{-1}\hat{\Lambda}_{z\delta_f}^{-1}\left(-\sum_k \hat{B}_z^k f_z^k - K_z e_z\right) \tag{19}$$

where $\hat{\Lambda}_{z_{\delta_f}}$ is assumed full rank, then the time derivative of the Lyapunov function V_3 becomes

$$V_3'|_{(16)} = -e_z^T K_z e_z \tag{20}$$

which is negative definite for any positive-definite K_z. This ensures that the equilibrium $e_z = 0$ of reduced subsystem (16) is stable in the sense of Lyapunov. By design of the fast actuator manifold δ_f^0, the special case $\delta_f^0|_{z^0}$ needed in the slowest timescale can now be determined as

$$\delta_f^0|_{z^0} = -G_{z\delta_f}^{-1}\hat{\Lambda}_{z\delta_f}^{-1}\sum_k \hat{B}_z^k f_z^k(x,\xi,z^0) \tag{21}$$

4. *Design of Fast Control in Fastest Timescale*

In the fastest timescale $t_\rho = (t/\rho)$, the fast controls u_f are selected such that the fast actuators δ_f reach their manifold δ_f^0 or, equivalently, fast actuator errors $e_{\delta_f} = \delta_f - \delta_f^0$ reach zero. Considering estimates of the unknown parameter matrices B_{δ_f} and $\Lambda_{\delta_f u_f}$, the reduced subsystem in the fastest timescale is

$$\check{e}_{\delta_f} = \hat{B}_{\delta_f} f_{\delta_f} + \hat{\Lambda}_{\delta_f u_f} G_{\delta_f u_f} u_f \tag{22}$$

A positive-definite candidate Lyapunov function for subsystem (22) is selected as

$$V_4 = \frac{1}{2} e_{\delta_f}^T e_{\delta_f} \tag{23}$$

Along the trajectories of reduced subsystem (22), the time derivative becomes

$$\check{V}_4|_{(22)} = e_{\delta_f}^T(\hat{B}_{\delta_f} f_{\delta_f} + \hat{\Lambda}_{\delta_f u_f} G_{\delta_f u_f} u_f) \tag{24}$$

If the fast control vector u_f is selected as

$$u_f = G_{\delta_f u_f}^{-1}\hat{\Lambda}_{\delta_f u_f}^{-1}(-\hat{B}_{\delta_f} f_{\delta_f} - K_{\delta_f} e_{\delta_f}) \tag{25}$$

where $\hat{\Lambda}_{\delta_f u_f}$ is assumed full rank, then the derivative of the Lyapunov function V_4 becomes

$$\check{V}_4|_{(22)} = -e_{\delta_f}^T K_{\delta_f} e_{\delta_f} \tag{26}$$

which is negative definite for any positive-definite K_{δ_f}. Thus, the equilibrium $e_{\delta_f} = 0$ of reduced subsystem (22) is stable in the sense of Lyapunov.

B. Selection of Parameter Update Laws and Ultimate Boundedness of Errors

This is the second stage in the control law development. It begins with constructing a composite Lyapunov function that includes the individual Lyapunov functions for the controller plus terms corresponding to parameter estimation errors. For a generic parameter matrix P and its estimate $\hat{P}$, the estimation error is $\tilde{P} := P - \hat{P}$. For the multiple-timescale system represented by Eq. (4), define parameter estimation error matrices $\tilde{B}_{xx} := B_{xx} - \hat{B}_{xx}$, $\tilde{B}_{xz} := B_{xz} - \hat{B}_{xz}$, $\tilde{\Lambda}_{x\delta_s} := \Lambda_{x\delta_s} - \hat{\Lambda}_{x\delta_s}$, $\tilde{\Lambda}_{x\delta_f} := \Lambda_{x\delta_f} - \hat{\Lambda}_{x\delta_f}$, $\tilde{B}_{\delta_s} := B_{\delta_s} - \hat{B}_{\delta_s}$, $\tilde{\Lambda}_{\delta_s u_s} := \Lambda_{\delta_s u_s} - \hat{\Lambda}_{\delta_s u_s}$, $\tilde{B}_z^k := B_z^k - \hat{B}_z^k$, $\tilde{\Lambda}_{z\delta_f} := \Lambda_{z\delta_f} - \hat{\Lambda}_{z\delta_f}$, $\tilde{B}_{\delta_f} := B_{\delta_f} - \hat{B}_{\delta_f}$, and $\tilde{\Lambda}_{\delta_f u_f} := \Lambda_{\delta_f u_f} - \hat{\Lambda}_{\delta_f u_f}$. A composite Lyapunov function for full-order system (4) is selected as

$$\begin{aligned} V_c = {} & \alpha_1 V_1 + \alpha_2 V_2 + \alpha_3 V_3 + \alpha_4 V_4 + \frac{1}{2}\alpha_5 \mathrm{tr}\left(\tilde{B}_{xx}^T \tilde{B}_{xx}\right) \\ & + \frac{1}{2}\alpha_6 \mathrm{tr}\left(\tilde{B}_{xz}^T \tilde{B}_{xz}\right) + \frac{1}{2}\alpha_7 \mathrm{tr}\left(\tilde{\Lambda}_{x\delta_s}^T \tilde{\Lambda}_{x\delta_s}\right) \\ & + \frac{1}{2}\alpha_8 \mathrm{tr}\left(\tilde{\Lambda}_{x\delta_f}^T \tilde{\Lambda}_{x\delta_f}\right) + \frac{1}{2}\alpha_9 \mathrm{tr}\left(\tilde{B}_{\delta_s}^T \tilde{B}_{\delta_s}\right) + \frac{1}{2}\alpha_{10} \mathrm{tr}\left(\tilde{\Lambda}_{\delta_s u_s}^T \tilde{\Lambda}_{\delta_s u_s}\right) \\ & + \frac{1}{2}\sum_k \alpha_{11k} \mathrm{tr}\left(\tilde{B}_z^{k^T} \tilde{B}_z^k\right) \\ & + \frac{1}{2}\alpha_{12} \mathrm{tr}\left(\tilde{\Lambda}_{z\delta_f}^T \tilde{\Lambda}_{z\delta_f}\right) + \frac{1}{2}\alpha_{13} \mathrm{tr}\left(\tilde{B}_{\delta_f}^T \tilde{B}_{\delta_f}\right) + \frac{1}{2}\alpha_{14} \mathrm{tr}\left(\tilde{\Lambda}_{\delta_f u_f}^T \tilde{\Lambda}_{\delta_f u_f}\right) \end{aligned} \tag{27}$$

where $\alpha_i > 0$; $i = 1, \ldots, 14$ represent the weights of the individual Lyapunov functions in the composite, and $\mathrm{tr}(A)$ denotes the trace of a matrix A. In terms of the individual elements of the parameter estimation error matrices, the composite Lyapunov function can be written as

$$\begin{aligned} V_c = {} & \alpha_1 V_1 + \alpha_2 V_2 + \alpha_3 V_3 + \alpha_4 V_4 + \frac{1}{2}\alpha_5 \sum_i \sum_j \tilde{b}_{xx_{ij}}^2 \\ & + \frac{1}{2}\alpha_6 \sum_i \sum_j \tilde{b}_{xz_{ij}}^2 + \frac{1}{2}\alpha_7 \sum_i \sum_j \tilde{\lambda}_{x\delta_{sij}}^2 \\ & + \frac{1}{2}\alpha_8 \sum_i \sum_j \tilde{\lambda}_{x\delta_{fij}}^2 + \frac{1}{2}\alpha_9 \sum_i \sum_j \tilde{b}_{\delta_{sij}}^2 + \frac{1}{2}\alpha_{10} \sum_i \sum_j \tilde{\lambda}_{\delta_s u_{sij}}^2 \\ & + \frac{1}{2}\sum_k \alpha_{11k} \sum_i \sum_j \tilde{b}_{z_{ij}}^{k^2} + \frac{1}{2}\alpha_{12} \sum_i \sum_j \tilde{\lambda}_{z\delta_{fij}}^2 \\ & + \frac{1}{2}\alpha_{13} \sum_i \sum_j \tilde{b}_{\delta_{fij}}^2 + \frac{1}{2}\alpha_{14} \sum_i \sum_j \tilde{\lambda}_{\delta_f u_{fij}}^2 \end{aligned} \tag{28}$$

For this choice of the Lyapunov function for full-order system (4), Theorem 1 gives sufficient conditions for ultimate boundedness of all of the errors: tracking errors, manifold errors, and parameter estimation errors.

Theorem 1: Suppose that the slow state tracking controller for the full-order nonlinear four-timescale system [Eq. (4)] is designed according to Eqs. (8), (9), (14), (19), and (25) using estimates of the unknown parameters. Suppose now that the estimates are updated according to the following laws:

$$\begin{aligned} \dot{\hat{b}}_{xx_{ij}} &= \frac{\alpha_1}{\alpha_5} e_{x_i} f_{xx_j} - \frac{\theta_1}{\alpha_5}\left(\hat{b}_{xx_{ij}} - b_{xx_{ij}}^0\right) \\ \dot{\hat{b}}_{xz_{ij}} &= \frac{\alpha_1}{\alpha_6} e_{x_i} (F_{xz} z^0)_j - \frac{\theta_2}{\alpha_6}\left(\hat{b}_{xz_{ij}} - b_{xz_{ij}}^0\right) \\ \dot{\hat{\lambda}}_{x\delta_{sij}} &= \frac{\alpha_1}{\alpha_7} e_{x_i} (G_{x\delta_s} \delta_s^0)_j - \frac{\theta_3}{\alpha_7}\left(\hat{\lambda}_{x\delta_{sij}} - \lambda_{x\delta_{sij}}^0\right) \\ \dot{\hat{\lambda}}_{x\delta_{fij}} &= \frac{\alpha_1}{\alpha_8} e_{x_i} (G_{x\delta_f} \delta_f^0|_{z^0})_j - \frac{\theta_4}{\alpha_8}\left(\hat{\lambda}_{x\delta_{fij}} - \lambda_{x\delta_{fij}}^0\right) \end{aligned} \tag{29}$$

$$\begin{aligned} \dot{\hat{b}}_{\delta_{sij}} &= \frac{\alpha_2}{\alpha_9} e_{\delta_{si}} f_{\delta_{sj}} - \frac{\theta_5}{\alpha_9}\left(\hat{b}_{\delta_{sij}} - b_{\delta_{sij}}^0\right) \\ \dot{\hat{\lambda}}_{\delta_s u_{sij}} &= \frac{\alpha_2}{\alpha_{10}} e_{\delta_{si}} (G_{\delta_s u_s} u_s)_j - \frac{\theta_6}{\alpha_{10}}\left(\hat{\lambda}_{\delta_s u_{sij}} - \lambda_{\delta_s u_{sij}}^0\right) \end{aligned} \tag{30}$$

$$\begin{aligned} \hat{b}_{z_{ij}}^{k\prime} &= \frac{\alpha_3}{\alpha_{11k}} e_{z_i} f_{z_j}^k - \frac{\theta_7}{\alpha_{11k}}\left(\hat{b}_{z_{ij}}^k - b_{z_{ij}}^k\right) \\ \hat{\lambda}_{z\delta_{fij}}' &= \frac{\alpha_3}{\alpha_{12}} e_{z_i} (G_{z\delta_f} \delta_f^0)_j - \frac{\theta_8}{\alpha_{12}}\left(\hat{\lambda}_{z\delta_{fij}} - \lambda_{z\delta_{fij}}^0\right) \end{aligned} \tag{31}$$

$$\begin{aligned} \check{\hat{b}}_{\delta_{fij}} &= \frac{\alpha_4}{\alpha_{13}} e_{\delta_{fi}} f_{\delta_{fj}} - \frac{\theta_9}{\alpha_{13}}\left(\hat{b}_{\delta_{fij}} - b_{\delta_{fij}}^0\right) \\ \check{\hat{\lambda}}_{\delta_f u_{fij}} &= \frac{\alpha_4}{\alpha_{14}} e_{\delta_{fi}} (G_{\delta_f u_f} u_f)_j - \frac{\theta_{10}}{\alpha_{14}}\left(\hat{\lambda}_{\delta_f u_{fij}} - \lambda_{\delta_f u_{fij}}^0\right) \end{aligned} \tag{32}$$

where y_i denotes the ith element of the column vector y; $\theta_i > 0$, $i = 1, \ldots, 10$ are estimator gains; and $b^0_{xx_{ij}}$, $b^0_{xz_{ij}}$, $\lambda^0_{x\delta_{sij}}$, $\lambda^0_{x\delta_{fij}}$, $b^0_{\delta_{sij}}$, $\lambda^0_{\delta_s u_{sij}}$, $b^{k^0}_{z_{ij}}$, $\lambda^0_{z\delta_{fij}}$, $b^0_{\delta_{fij}}$, and $\lambda^0_{\delta_f u_{fij}}$ are additional design variables. It is now possible to choose the controller gains, estimator gains, and other design variables such that the tracking errors, the manifold errors, and the parameter estimation errors remain ultimately bounded.

The detailed proof can be found in Ref. [33]. The essential steps of the proof are presented in Appendix B. Note that selections of the parameter update laws are similar to those of Dong and Kuhnert [34]. Each update law has one term to cancel the associated error appearing adjacent to the time derivative of the corresponding estimate. The second part drives the estimate to a specified final value at a specified rate of a first-order dynamic. The final values of the estimates are specified by the design variables $b^0_{xx_{ij}}$, $b^0_{xz_{ij}}$, $\lambda^0_{x\delta_{sij}}$, etc.; and the rates of the first-order dynamics are specified by the estimator gains θ_i; $i = 1, 2, \ldots, 10$.

C. Summary of Multiple-Timescale Controller Development

The design steps of the multiple-timescale controller developed in Secs. III.A and III.B are summarized in Table 1.

D. Comparison with Cascaded Nonlinear Dynamic Inversion Controller Without Using Explicit Timescale Separation

An NDI controller without explicit classification of the states and the actuators as slow and fast is designed for the purpose of comparing with the GSP controller. NDI is a well-known technique in aircraft flight control [35–37] that was seen to achieve better performance than a gain-scheduled linear controller with a similar level of design effort [35]. Both noncascaded and cascaded versions of NDI can be found in the literature [31,32]. The cascaded version of NDI develops the controller structure in nested loops under the assumption of a timescale separation between the inner and the outer loops; i.e., the inner loop is faster than the outer loop. However, unlike the GSP approach, this method neither constructs reduced subsystems nor uses a Lyapunov framework explicitly in different timescales. The design variables are selected using feedback linearization in successive loop closures. The derivatives of the design variables are needed for subsequent steps, and they are estimated using first-order low-pass filters.

Table 1 Design Steps of the Multiple-Timescale Controller Using GSP

Step	Description
1	Compute the tracking error for the kinematic slow states: $e_\xi = \xi - \xi_r$. Choose gain K_ξ.
	Compute the manifold of the fast states: $z^0 = F^{-1}_{\xi z}(\dot{\xi}_r - K_\xi e_\xi)$.
2	Compute the manifold error for the fast states: $e_z = z - z^0$. Choose gain K_z.
	Compute the manifold of the fast actuators: $\delta^0_f = G^{-1}_{z\delta_f}\hat{\Lambda}^{-1}_{z\delta_f}\left(-\sum_k \hat{B}^k_z f^k_z - K_z e_z\right)$.
3	Compute the fast actuator manifold error: $e_{\delta_f} = \delta_f - \delta^0_f$. Choose gain K_{δ_f}.
	Compute the fast control: $u_f = G^{-1}_{\delta_f u_f}\hat{\Lambda}^{-1}_{\delta_f u_f}\left(-\hat{B}_{\delta_f} f_{\delta_f} - K_{\delta_f} e_{\delta_f}\right)$.
4	Compute a special case of the fast actuator manifold: $\delta^0_f\|_{z^0} = -G^{-1}_{z\delta_f}\hat{\Lambda}^{-1}_{z\delta_f}\sum_k \hat{B}^k_z f^k_z(x, \xi, z^0)$.
	Compute the tracking error for the kinetic slow states: $e_x = x - x_r$. Choose gain K_x.
	Compute the manifold of the slow actuators: $\delta^0_s = G^{-1}_{x\delta_s}\hat{\Lambda}^{-1}_{x_{\delta_s}}(\dot{x}_r - \hat{B}_{xx} f_{xx} - \hat{B}_{xz} F_{xz} z^0 - \hat{\Lambda}_{x\delta_f} G_{x\delta_f}\delta^0_f\|_{z^0} - K_x e_x)$.
5	Compute the slow actuator manifold error: $e_{\delta_s} = \delta_s - \delta^0_s$. Choose gain K_{δ_s}.
	Compute the slow control $u_s = G^{-1}_{\delta_s u_s}\hat{\Lambda}^{-1}_{\delta_s u_s}\left(-\hat{B}_{\delta_s} f_{\delta_s} - K_{\delta_s} e_{\delta_s}\right)$.
6	Choose weights α_i, estimator gains θ_i, and final values of estimates $b^0_{xx_{ij}}$, $b^0_{xz_{ij}}$, $\lambda^0_{x\delta_{sij}}$, etc.
	Update the estimates using Eqs. (29–32).

For the control objective stated in Sec. II, it is not convenient to apply cascaded NDI directly on the mathematical form of the full-order system [Eq. (3)] with omission of the timescale separation parameters σ, ε, and ρ. If the control objective is the tracking of the kinematic states ξ only, it is convenient to treat x as known from measurement and use the $\dot{\xi}$, $\dot{z}$, and $\dot{\delta}_f$ equations to design a cascaded NDI controller. Alternatively, if the control objective is the tracking of the kinetic states x only, it is convenient to treat ξ, z, and δ_f as known from measurement and use the $\dot{x}$ and $\dot{\delta}_s$ equations to design another NDI controller. For the aircraft problem, if only the Euler angles are to be tracked, a cascaded NDI controller can command the aerodynamic controls under the assumption that velocity is somehow stabilized by a separate controller. Alternatively, if only the velocity is to be tracked, a cascaded NDI controller can command throttle with the assumption that the Euler angles are somehow stabilized by a separate controller. However, when both the kinetic and kinematic states are to be tracked by a single controller, a way to implement cascaded NDI is as follows. System (3) without the timescale parameters σ, ε, and ρ can be rewritten as

$$
\begin{aligned}
\dot{e}_\xi &= F_{\xi z}(.)z - \dot{\xi}_r \\
\begin{bmatrix} \dot{z} \\ \dot{e}_x \end{bmatrix} &= \begin{bmatrix} \sum_k B^k_z f^k_z(.) + \gamma_z(.) \\ B_{xx} f_{xx}(.) + B_{xz} F_{xz}(.) + \gamma_x(.) - \dot{x}_r \end{bmatrix} \\
&\quad + \begin{bmatrix} 0 & \Lambda_{z\delta_f} G_{z\delta_f}(.) \\ \Lambda_{x\delta_s} G_{x\delta_s}(.) & \Lambda_{x\delta_f} G_{x\delta_f}(.) \end{bmatrix}\delta \\
\dot{\delta} &= B_\delta f_\delta(\delta) + \Lambda_{\delta u} G_{\delta u}(\delta) u
\end{aligned} \tag{33}
$$

where

$$
\delta := \begin{bmatrix} \delta_s \\ \delta_f \end{bmatrix}, \quad B_\delta := \begin{bmatrix} B_{\delta_s} & 0 \\ 0 & B_{\delta_f} \end{bmatrix}, \quad f_\delta(.) := \begin{bmatrix} f_{\delta_s}(.) \\ f_{\delta_f}(.) \end{bmatrix},
$$

$$
\Lambda_{\delta u} := \begin{bmatrix} \Lambda_{\delta_s u_s} & 0 \\ 0 & \Lambda_{\delta_f u_f} \end{bmatrix}, \quad G_{\delta u} := \begin{bmatrix} G_{\delta_s u_s} & 0 \\ 0 & G_{\delta_f u_f} \end{bmatrix},
$$

$$
\text{and } u := \begin{bmatrix} u_s \\ u_f \end{bmatrix}
$$

Using the estimates of constant but unknown parameters, the controller structure is

$$
\begin{aligned}
e_\xi &= \xi - \xi_r \\
z_d &= F_{\xi z}(.)^{-1}(\dot{\xi}_r - K_\xi e_\xi) \\
T_z \dot{z}_c + z_c &= z_d; z_c(0) = z_d(0) \\
e_z &= z - z_c \\
e_x &= x - x_r \\
\delta_d &= \begin{bmatrix} 0 & \hat{\Lambda}_{z\delta_f} G_{z\delta_f}(.) \\ \hat{\Lambda}_{x\delta_s} G_{x\delta_s}(.) & \hat{\Lambda}_{x\delta_f} G_{x\delta_f}(.) \end{bmatrix}^{-1} \\
&\quad \left\{ \begin{bmatrix} \dot{z}_c - \sum_k \hat{B}^k_z f^k_z(.) \\ \dot{x}_r - \hat{B}_{xx} f_{xx}(.) - \hat{B}_{xz} F_{xz}(.) \end{bmatrix} - \begin{bmatrix} K_z e_z \\ K_x e_x \end{bmatrix} \right\} \\
T_\delta \dot{\delta}_c + \delta_c &= \delta_d; \delta_c(0) = \delta_d(0) \\
e_\delta &= \delta - \delta_c \\
u &= G_{\delta u}(\delta)^{-1}\hat{\Lambda}^{-1}_{\delta u}(\dot{\delta}_c - \hat{B}_\delta f_\delta(\delta) - K_\delta e_\delta)
\end{aligned} \tag{34}
$$

It can be seen in Eq. (34) that the desired value z_d of the states z and the desired value δ_d of the actuators δ result from dynamic inversion, canceling the nonlinearities and imposing linear dynamics. The desired values z_d and δ_d are passed through first-order filters with

time constants captured in matrices T_z and T_δ. The filtered outputs z_c and δ_c are used in the subsequent stages. Compared to the multiple-timescale method, this controller has the additional design variables of filter time-constant matrices T_z and T_δ. The parameter update laws for this controller are similar to that of the multiple-timescale controller, except for the fact that the actual values of the states and actuators are used instead of manifolds wherever applicable.

IV. Numerical Results

This section compares the performance of the two nonlinear slow state tracking controllers developed in Sec. III: the multiple-timescale controller using GSP, and the cascaded NDI controller. The simulation is a non-real-time nonlinear 6-DOF generic F-16A. The evaluation maneuver is a large-amplitude longitudinal and lateral/directional maneuver that is a combination of those used in previous work by Saha et al. [25] and Saha and Valasek [38]; but here, the pitch attitude angle is commanded instead of the body-axis pitch rate. From trim, the aircraft is commanded to perform a steep climb. During the climb, the pitch attitude angle reaches a maximum to 80 deg in 10 s, stays at 80 deg for another 10 s, followed by a further 10 s for the nose to level out. No banking or change of heading angle is commanded during the climb. After the climb is complete, the aircraft is commanded to perform a 90 deg left turn followed by a 90 deg right turn [26]. The heading angle is desired to change by 90 deg in 15 s for each turn. The bank angle and the pitch attitude angle associated with each turn are commanded to reach a maximum from zero, and then they come back to zero as the turn is complete. The maximum bank angle and pitch attitude angle associated with each turn are 75 and 20 deg, respectively. The velocity is commanded to be close to the trim value throughout the maneuver. The simulation is run for 150 s for both controllers.

The flight condition is a steady, level, $1g$ trim flight at Mach 0.7 and 15,000 ft. The trim angle of attack and elevator deflection are 0.9 and -1.6 deg, respectively. The thrust at trim is 3265.0 lbf, which is 18.34% of the maximum military thrust of 17,800 lbf. The pitch attitude angle at trim is the same as the trim angle of attack. All other angles, rates, and control surface deflections are zero at trim.

Both controllers are applied to a plant subject to uncertainties in inertias, control derivatives, and engine time constant. The initial estimate of each of the inertias I_{xx}, I_{yy}, I_{zz}, and I_{xz} is assumed to be 15% below its actual value. The initial estimate of each of the control derivatives $C_{x_{\delta_e}}$, $C_{y_{\delta_a}}$, $C_{y_{\delta_r}}$, $C_{z_{\delta_e}}$, $C_{m_{\delta_e}}$, $C_{l_{\delta_a}}$, $C_{l_{\delta_r}}$, $C_{n_{\delta_a}}$, and $C_{n_{\delta_r}}$ is assumed to be 20% below its actual value. The engine time constant is assumed to be 25% above its actual value.

A. Selection of the Numerical Values of the Control Gains

The gain matrices must be positive definite in order to guarantee the stability of each reduced subsystem. Theorem 1 shows that the gains can be selected such that errors remain ultimately bounded. Equation (B6) in the proof of Theorem 1 presented in Appendix B suggests that the gain matrices should be "large enough" such that β_i; $i = 1, \ldots, 5$ are positive, and each one of them exceeds the factor (μ/θ_r^2). In practice, it may be difficult to know all of the values needed to compute (μ/θ_r^2). For the present work, initial values for the gain matrices were chosen and subsequently adjusted, depending on the response of the corresponding states. The gains for the multiple-timescale controller based on GSP are selected as $K_x = 25$, $K_\xi = \text{diag}[2, 2, 1]$, $K_{\delta_s} = 0.01$, $K_z = \text{diag}[25, 10, 5]$, and $K_{\delta_f} = \text{diag}[3, 2, 2]$. The gains for the cascaded nonlinear dynamic inversion controller are $K_x = 10$, $K_\xi = \text{diag}[2.5, 1.5, 1]$, $K_{\delta_s} = 0.01$, $K_z = \text{diag}[15, 15, 15]$, and $K_{\delta_f} = \text{diag}[1, 1, 1]$.

B. Selection of Numerical Values of Parameter Estimator Gains

The gains θ_i are included in the factor μ of (μ/θ_r^2) in Eq. (B4) in Appendix B, which presents the proof of Theorem 1. According to Eq. (B4), the gains θ_i should be "small enough" such that β_i can exceed (μ/θ_r^2) without making the control gains too large. At the same time, the gains θ_i should be large enough such that each one of $(\theta_1/2)$, $(\theta_2/2)$, $(\theta_3/2)$, $(\theta_4/2)$, $(\theta_5/2\sigma)$. $(\theta_6/2\sigma)$, $(\theta_7/2\varepsilon)$, $(\theta_8/2\varepsilon)$, $(\theta_9/2\rho)$, and $(\theta_{10}/2\rho)$ can exceed (μ/θ_r^2). Because of the coupling in the equations, the analytical computation of suitable values for θ_i for guaranteed stability is difficult. However, the gains θ_i physically represent the rate at which the parameter estimates converge to their assigned final values and can be adjusted by inspecting at what rate the estimates respond. Some of the gains α_i; $i = 1, 2, 3$ in the parameter estimator are significantly smaller than the other gains θ_i; $i = 4, \ldots, 8$ and are used to cancel the error terms in the parameter update laws. In theory, they should be positive so that the composite Lyapunov function is positive definite. However, even when each of these gains is set to zero in simulation, the tracking of aircraft states and controls is very similar to the case of small positive magnitudes of the gains. Only some of the parameter estimates are observed to not evolve at all, but this is not as important as the tracking. Because the gains α_1, α_2, and α_3 multiply error terms, the magnitude of these gains being small ensures that the contributions of error terms in the parameter update laws are small, even for the case in which the errors themselves become large.

The parameter estimator gains are selected as $\alpha_1 = 10^{-13}$, $\alpha_2 = 10^{-14}$, $\alpha_3 = 10^{-15}$, $\alpha_8 = 1$, $\alpha_9 = 1$, $\alpha_{10} = 1$, $\alpha_{111} = 1$, $\alpha_{112} = 1$, $\alpha_{12} = 1$, and $\theta_i = 0.1$; $i = 4, 5, 6, 7, 8$. The design variables corresponding to the final value of the estimates in the parameter update laws are chosen such that the inertias, control derivatives, and engine time constant are 5% above the actual values.

C. Selection of Numerical Values of Filter Time Constants for the Cascaded NDI

The inherent assumption for the cascaded NDI to work according to Eq. (33) is that the innermost loop of actuators δ is the fastest, the outermost loop of the kinematic states ξ is the slowest, and the middle loop of the states z and x has an intermediate rate of response. To enforce this separation, each filter for δ is selected to respond 10 times faster than each filter for z. The filter time constants for the cascaded NDI controller are selected as $T_z = \text{diag}[1, 1, 1]$ and $T_\delta = \text{diag}[0.1, 0.1, 0.1, 0.1]$.

D. Comparison of the Two Controllers

For both the GSP and NDI controllers, Figs. 2–7 show the time histories of the states and controls and Figs. 8–14 show the evolution of the uncertain parameters. The notations for the parameter matrices are as follows: $B_z^1 := [B_{ij}]_{3\times5}$, $B_z^2 := [S_{ij}]_{3\times3}$, and $\Lambda_{z\delta_f} := [L_{ij}]_{3\times3}$. The mathematical expressions of the matrices are derived in Appendix A.

The multiple-timescale GSP and the cascaded NDI controllers produce similar performances in some aspects and significant differences in other aspects. Figures 8–14 show that the profiles of the estimates are different in some cases but the difference in magnitude is small. The parameter estimation errors remain bounded for both controllers, with the B matrix (which is obtained by multiplying the inertia matrix with its inverse) having estimation errors that are acceptably small in magnitude. Figures 4 and 5 show that the Euler angles and the body-axis angular rates are almost the same for both controllers. Both controllers are able to achieve good tracking of the kinematic angles, even though they use the elevator, aileron, and rudder somewhat differently, as seen in Fig. 7. The control surface deflections are well within their position and rate limits for both controllers. The angle of attack remains within acceptable limits for both controllers, but it is slightly larger for the NDI. Sideslip angles are within 6 deg for both controllers.

The significant difference between the two controllers concerns the velocity response. Between the completion of the climb and the initiation of the left turn, the maneuver has a gap of 10 s to allow the velocity to return to the reference. It is seen from Fig. 2 that the velocity initially drops from its trim value of 800 ft/s to less than 500 ft/s during the climb. The GSP controller is able to recover velocity rapidly after the climb. There is also a loss of velocity for each 90 deg turn, but the loss remains within 100 ft/s and is recovered as soon as each turn is complete. The cascaded NDI controller is not able to recover even half of the lost velocity in more than 100 s after the climb. In addition, some of the recovered velocity is lost during the turns and requires additional time to be recovered again. The throttle response in Fig. 6 shows that the GSP controller commands 100% throttle for some time after the climb or turn is

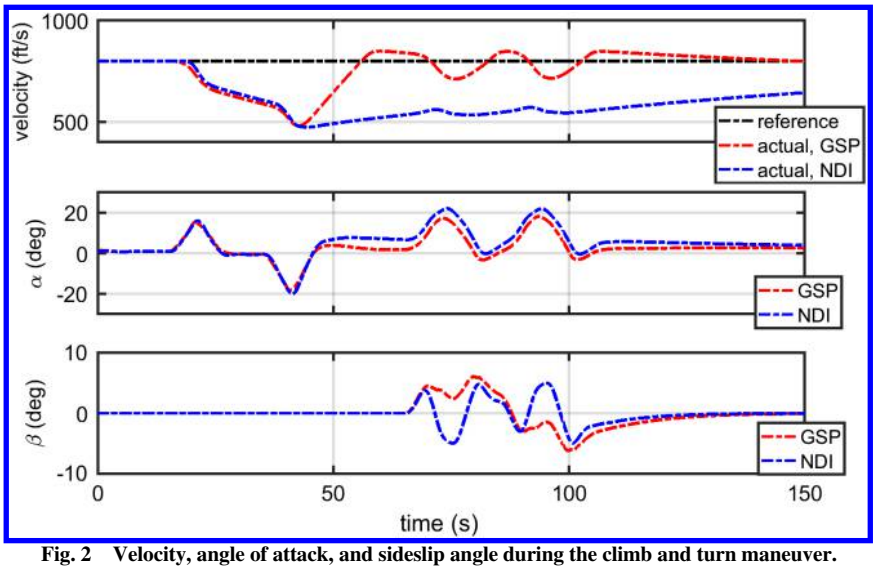

Fig. 2 Velocity, angle of attack, and sideslip angle during the climb and turn maneuver.

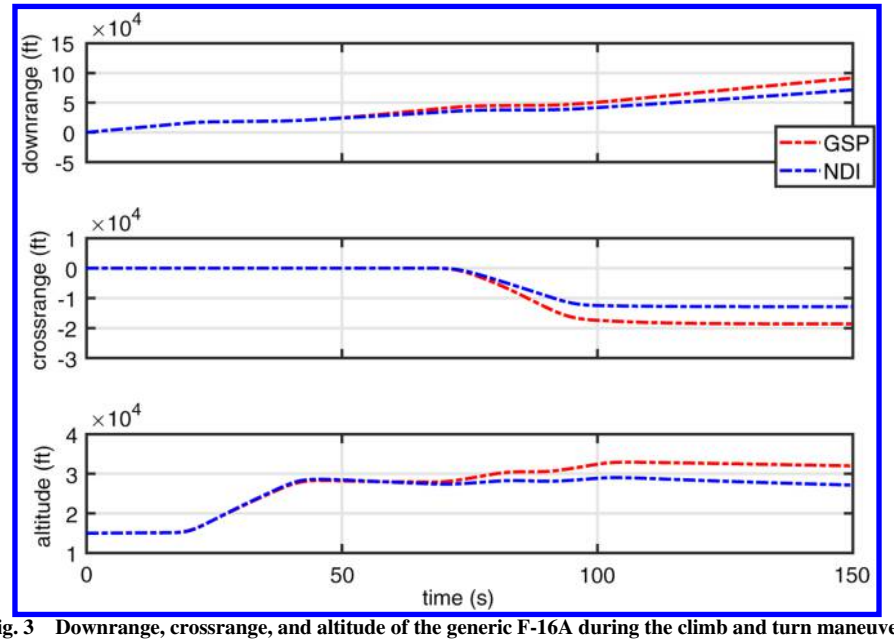

Fig. 3 Downrange, crossrange, and altitude of the generic F-16A during the climb and turn maneuver.

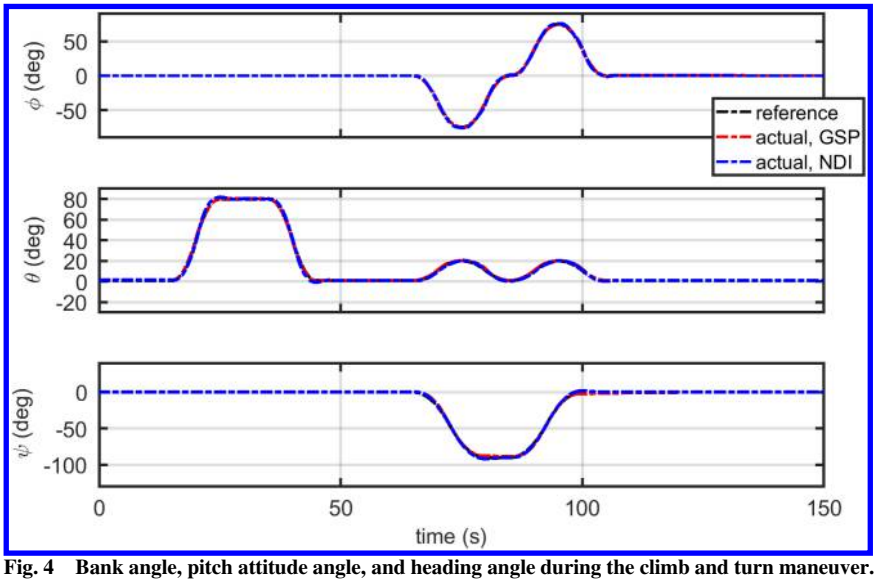

Fig. 4 Bank angle, pitch attitude angle, and heading angle during the climb and turn maneuver.

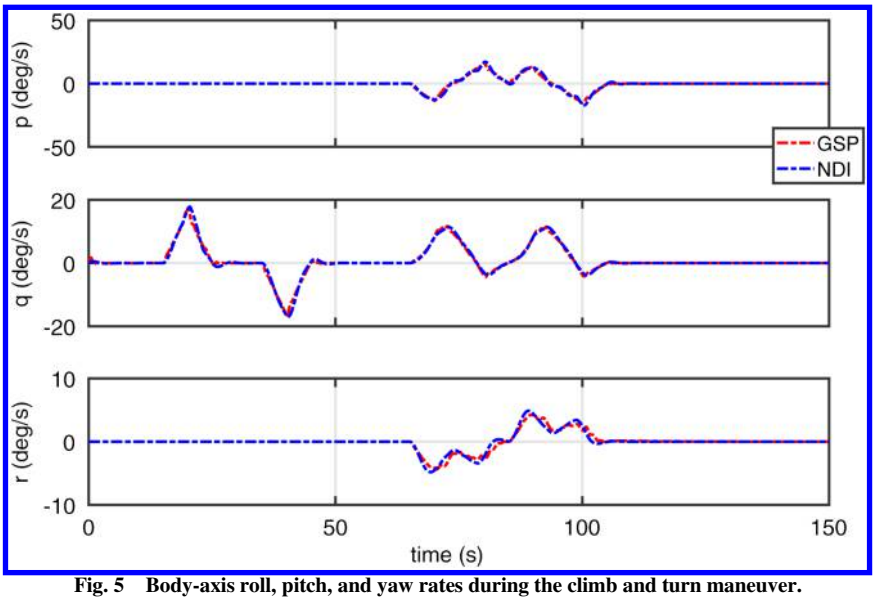

Fig. 5 Body-axis roll, pitch, and yaw rates during the climb and turn maneuver.

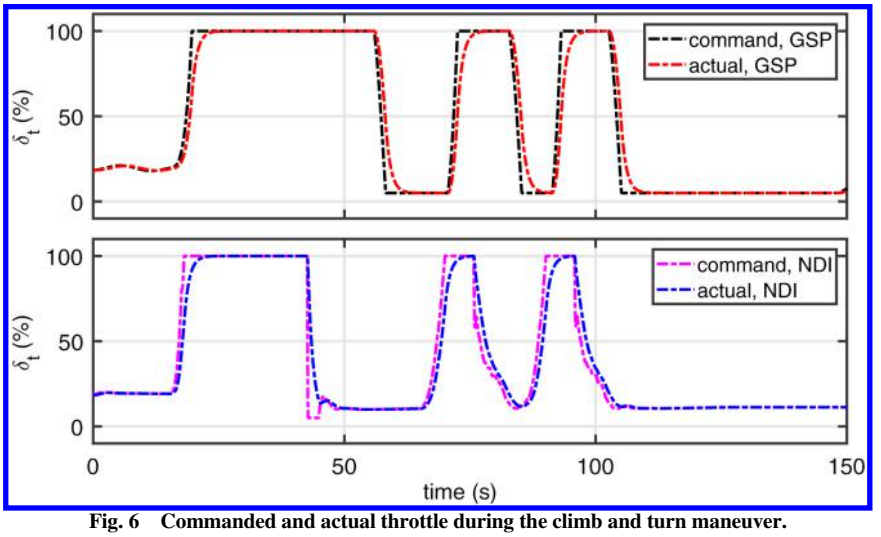

Fig. 6 Commanded and actual throttle during the climb and turn maneuver.

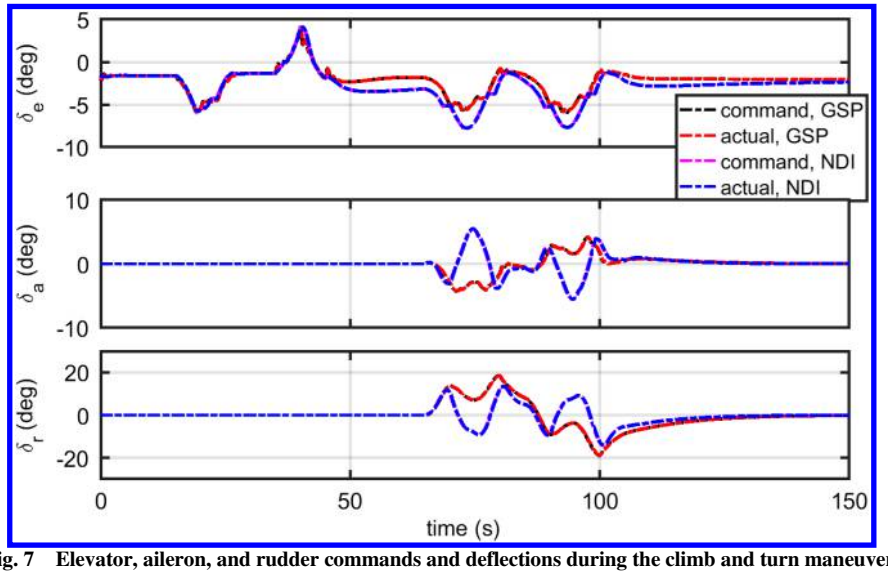

Fig. 7 Elevator, aileron, and rudder commands and deflections during the climb and turn maneuver.

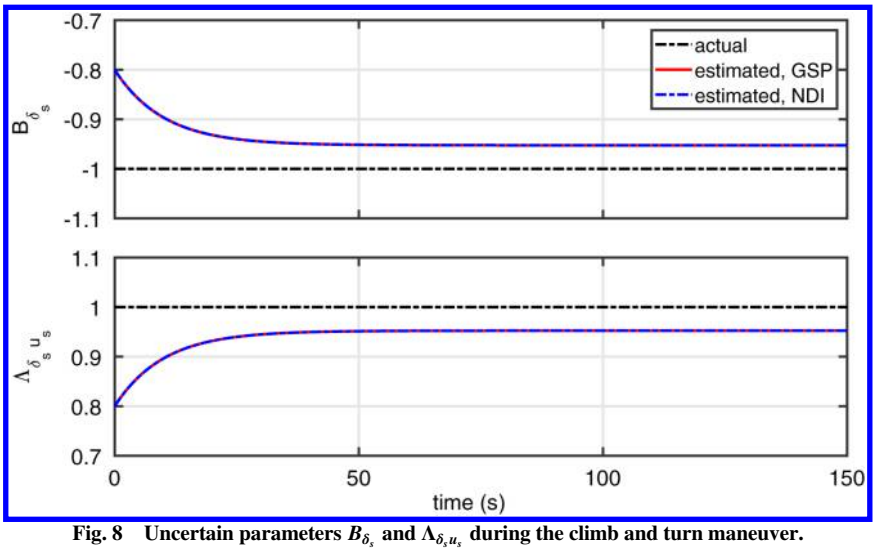

Fig. 8 Uncertain parameters B_{δ_s} and $\Lambda_{\delta_s u_s}$ during the climb and turn maneuver.

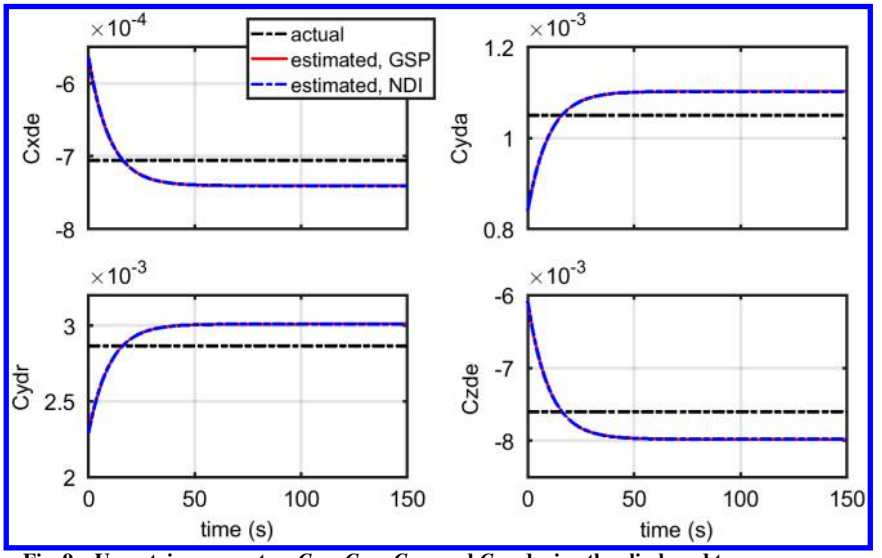

Fig. 9 Uncertain parameters $C_{x_{\delta_e}}$, $C_{y_{\delta_a}}$, $C_{y_{\delta_r}}$, and $C_{z_{\delta_e}}$ during the climb and turn maneuver.

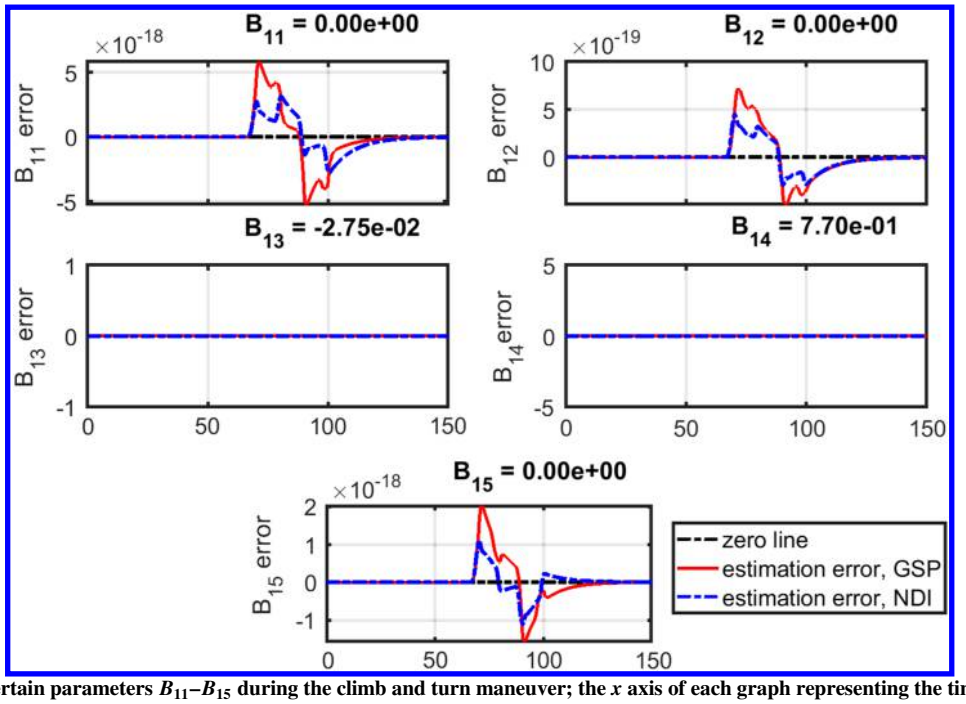

Fig. 10 Uncertain parameters B_{11}–B_{15} during the climb and turn maneuver; the x axis of each graph representing the time in seconds.

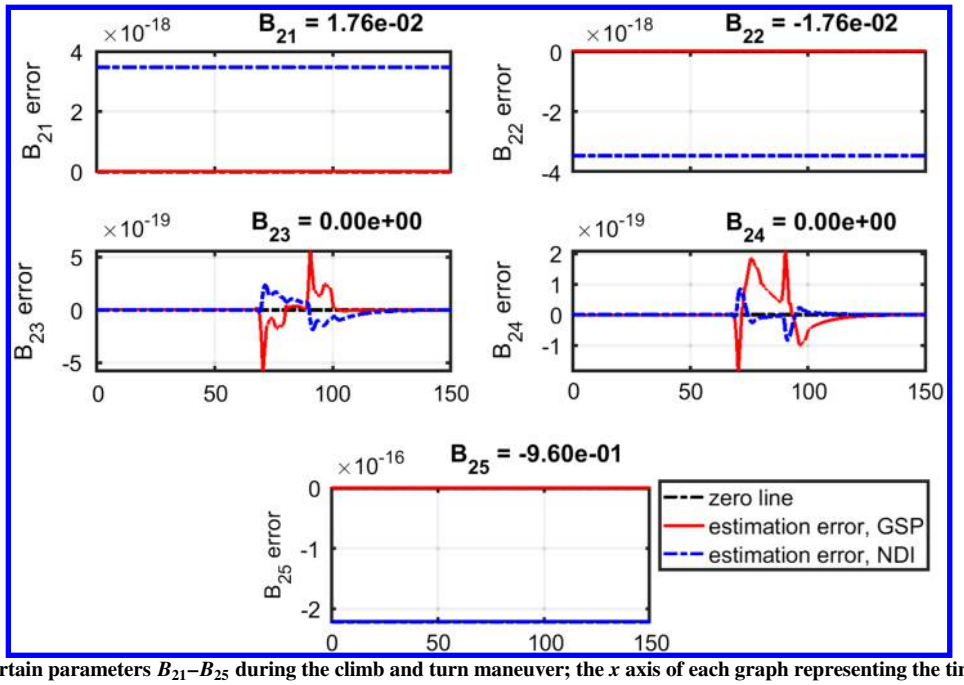

Fig. 11 Uncertain parameters B_{21}–B_{25} during the climb and turn maneuver; the x axis of each graph representing the time in seconds.

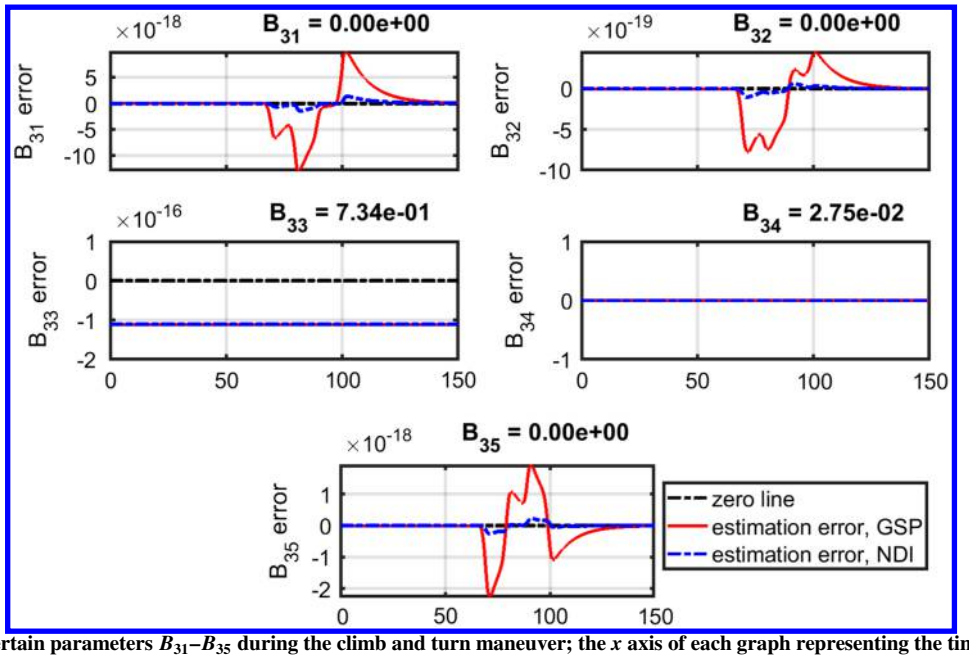

Fig. 12 Uncertain parameters B_{31}–B_{35} during the climb and turn maneuver; the x axis of each graph representing the time in seconds.

completed in order to recover the lost velocity. By comparison, the NDI controller reduces throttle as soon as the climb or turn is complete. Figure 3 shows a difference in the altitude profiles for the two different controllers. The GSP controller leads to climbing turns with a noticeable change in altitude during each turn. On the other hand, the gain in altitude for each turn is small for the NDI controller. Furthermore, the NDI controller leads to a decrease in altitude and an increase in velocity from $t = 110$ s onward. It is to be noted that, during this period, there is still a significant error in velocity, the throttle is already reduced, and the pitch attitude angle is close to zero. It can be inferred that the aircraft effectively tries to regain velocity by dropping altitude while keeping the nose close to horizontal. This is not the case with the GSP controller, for which the velocity has exceeded the trim value during turn, and it slowly decreases to trim from $t = 110$ s onward. Figure 3 also shows that the aircraft traverses a longer distance during the turns under GSP control as compared to cascaded NDI control because of the higher velocity achieved with the GSP controller.

The appreciable difference in the velocity response can be attributed to how the cascaded NDI is formulated for both kinetic and kinematic state tracking. The formulation in Eq. (33) inherently assumes that all of the actuators forming the innermost loop are faster than the states. This is not a good assumption when the real system has both slow and fast actuators, and the slow actuator is slower than the fast state. For example, the throttle for an aircraft responds slower than the body-axis angular rates, and this information is not captured accurately by the cascaded NDI. This suggests that, for an aircraft control objective of tracking both velocity and Euler angles, the multiple timescale GSP controller is able to make better use of the physical insight into aircraft dynamics, and therefore achieves better control of velocity.

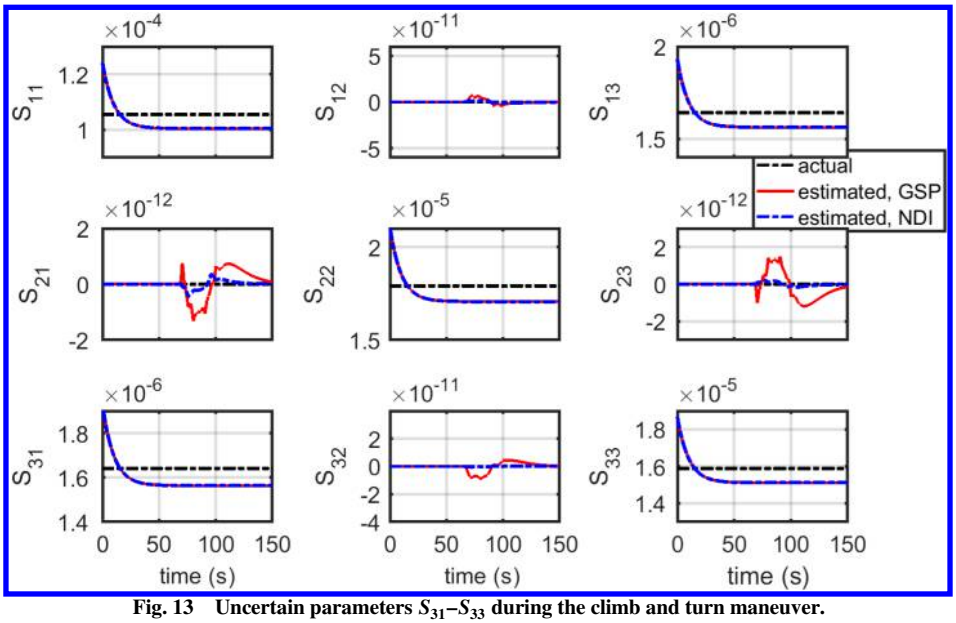

Fig. 13 Uncertain parameters S_{31}–S_{33} during the climb and turn maneuver.

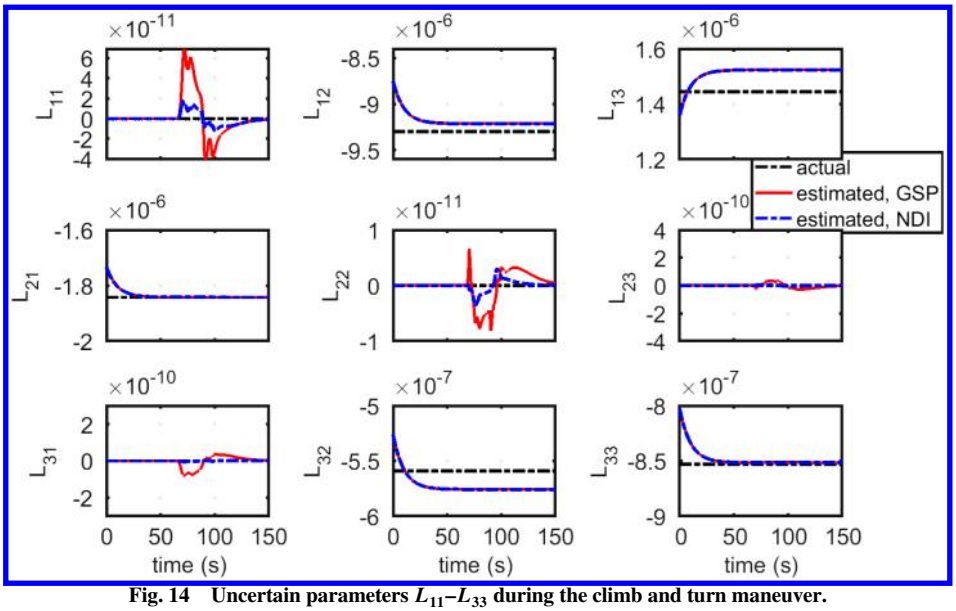

Fig. 14 Uncertain parameters L_{11}–L_{33} during the climb and turn maneuver.

V. Conclusions

This paper developed a multiple-timescale slow state tracking nonlinear controller to accomplish large-amplitude combined longitudinal and lateral/directional maneuvers of a nonlinear six-degree-of-freedom aircraft modeled with uncertainties in inertias, control derivatives, and engine time constant. Tracking errors, manifold errors, and parameter estimation errors were proven to be ultimately bounded; and the magnitude of each error was made arbitrarily small with suitable choices of gains. The controller was able to achieve slow state tracking even though the initial estimates of all of the unknown parameters were off by a reasonable amount. The angle of attack and sideslip angle were neither tracked nor used as intermediate controls, but they remain bounded and within acceptable limits. Gains and other design variables in the parameter update laws were chosen such that each unknown parameter multiplying a control signal never became zero, and so there was no singularity with respect to the controls.

The results presented in the paper compared the multiple-timescale nonlinear controller with a cascaded nonlinear dynamic inversion controller. Both controllers tracked the Euler angles adequately, but the former achieved better tracking of velocity due to an explicit distinction of the states, and especially the actuators, as slow and fast by means of timescale separation parameters. As a consequence, it was able to better use a physical insight into the dynamics. The geometric singular perturbation approach is judged to be a suitable candidate for aircraft systems with slow and fast states, as well as slow and fast actuators.

Appendix A: Vector Functions, Matrix Functions, and Parameter Matrices for a Nonlinear Six-Degree-of-Freedom Aircraft

The vectors and matrices used for control law development can be derived from the six kinetic and six kinematic equations of a nonlinear 6-DOF aircraft. The nonlinear 6-DOF generic F-16A model with the definitions of all the states, parameters, and aerodynamic stability and control derivatives were contained in the work of Stevens and Lewis [39]:

$$
\begin{aligned}
\dot{v}_A &= \frac{1}{m}[\cos\alpha\cos\beta(-mg\sin\theta + T_m\delta_t + F_{A_x}) \\
&\quad + \sin\beta(mg\cos\theta\sin\phi + F_{A_y}) \\
&\quad + \sin\alpha\cos\beta(mg\cos\theta\cos\phi + F_{A_z})] \\
\dot{\alpha} &= q - p\cos\alpha\tan\beta - r\sin\alpha\tan\beta \\
&\quad - \frac{\sin\alpha}{mv_A\cos\beta}(-mg\sin\theta + T_m\delta_t + F_{A_x}) \\
&\quad + \frac{\cos\alpha}{mv_A\cos\beta}(mg\cos\theta\cos\phi + F_{A_z}) \\
\dot{\beta} &= p\sin\alpha - r\cos\alpha - \frac{\sin\beta\cos\alpha}{mv_A}(-mg\sin\theta + T_m\delta_t + F_{A_x}) \\
&\quad + \frac{\cos\beta}{mv_A}(mg\cos\theta\sin\phi + F_{A_y}) \\
&\quad - \frac{\sin\beta\sin\alpha}{mv_A}(mg\cos\theta\cos\phi + F_{A_z}) \\
I_{xx}\dot{p} &= (I_{yy} - I_{zz})qr + I_{xz}(\dot{r} + pq) + L_A \\
I_{yy}\dot{q} &= (I_{zz} - I_{xx})rp + I_{xz}(r^2 - p^2) + M_A \\
I_{zz}\dot{r} &= (I_{xx} - I_{yy})pq + I_{xz}(\dot{p} - qr) + N_A \\
\dot{\phi} &= p + \tan\theta(q\sin\phi + r\cos\phi) \\
\dot{\theta} &= q\cos\phi - r\sin\phi \\
\dot{\psi} &= (q\sin\phi + r\cos\phi)\sec\theta \\
\dot{x}_N &= v_A[\cos\alpha\cos\beta\cos\theta\cos\psi + \sin\beta(\sin\phi\cos\psi\sin\theta - \cos\phi\sin\psi) \\
&\quad + \sin\alpha\cos\beta(\cos\phi\sin\theta\cos\psi + \sin\phi\sin\psi)] \\
\dot{y}_N &= v_A[\cos\alpha\cos\beta\cos\theta\sin\psi + \sin\beta(\sin\phi\sin\psi\sin\theta + \cos\phi\cos\psi) \\
&\quad + \sin\alpha\cos\beta(\cos\phi\sin\theta\sin\psi - \sin\phi\cos\psi)] \\
\dot{h} &= v_A(\cos\alpha\cos\beta\sin\theta - \sin\beta\sin\phi\cos\theta - \sin\alpha\cos\beta\cos\phi\cos\theta)
\end{aligned} \tag{A1}
$$

The body-axis aerodynamic forces and moments are modeled using component buildup as

$$
\begin{aligned}
F_{A_x} &= \left[C_x(\alpha,\delta_e) + C_{x_q}\frac{q\bar{c}}{2v_A}\right]\bar{q}S \\
F_{A_y} &= \left[C_{y_\beta}\beta + C_{y_p}\frac{pb}{2v_A} + C_{y_r}\frac{rb}{2v_A} + C_{y_{\delta_a}}\delta_a + C_{y_{\delta_r}}\delta_r\right]\bar{q}S \\
F_{A_z} &= \left[C_z(\alpha,\beta) + C_{z_q}\frac{q\bar{c}}{2v_A} + C_{z_{\delta_e}}\delta_e\right]\bar{q}S \\
L_A &= \left[C_l(\alpha,\beta) + C_{l_p}\frac{pb}{2v_A} + C_{l_r}\frac{rb}{2v_A} + C_{l_{\delta_a}}\delta_a + C_{l_{\delta_r}}\delta_r\right]\bar{q}Sb \\
M_A &= \left[C_m(\alpha,\delta_e) + C_{m_q}\frac{q\bar{c}}{2v_A} + \frac{x_{cg_r} - x_{\mathrm{cg}}}{\bar{c}}\right. \\
&\quad \left.\times\left(C_z(\alpha,\beta) + C_{z_q}\frac{q\bar{c}}{2v_A} + C_{z_{\delta_e}}\delta_e\right)\right]\bar{q}S\bar{c} \\
N_A &= \left[C_n(\alpha,\beta) + C_{n_p}\frac{pb}{2v_A} + C_{n_r}\frac{rb}{2v_A} + C_{n_{\delta_a}}\delta_a + C_{n_{\delta_r}}\delta_r\right. \\
&\quad + \frac{x_{\mathrm{cg}_r} - x_{\mathrm{cg}}}{b}\left(C_{y_\beta}\beta + C_{y_p}\frac{pb}{2v_A} + C_{y_r}\frac{rb}{2v_A}\right. \\
&\quad \left.\left. + C_{y_{\delta_a}}\delta_a + C_{y_{\delta_r}}\delta_r\right)\right]\bar{q}Sb
\end{aligned} \tag{A2}
$$

The aerodynamic database contains the coefficients $C_x(.)$, $C_z(.)$, $C_l(.)$, $C_m(.)$, and $C_n(.)$ as lookup tables for -10 deg $\le \alpha \le 45$ deg, -30 deg $\le \beta \le 30$ deg, and -25 deg $\le \delta_e \le 25$ deg. For values of α, β, and δ_e not included or outside the range, the nonlinear 6-DOF simulation has routines for interpolation and extrapolation. Using the data from the lookup tables, the force coefficient C_x and the moment coefficient C_m are approximated using linear least squares. The approximated forms are

$$
\begin{aligned}
C_x(\alpha,\delta_e) &\approx C_{x_0} + C_{x_\alpha}\alpha + C_{x_{\delta_e}}\delta_e \\
C_m(\alpha,\delta_e) &\approx C_{m_0} + C_{m_\alpha}\alpha + C_{m_{\delta_e}}\delta_e
\end{aligned} \tag{A3}
$$

where C_{x_0}, C_{x_α}, $C_{x_{\delta_e}}$, C_{m_0}, C_{m_α}, and $C_{m_{\delta_e}}$ are least square solutions.

The aerodynamic database provides the control derivatives $C_{l_{\delta_a}}$, $C_{l_{\delta_r}}$, $C_{n_{\delta_a}}$, and $C_{n_{\delta_r}}$ as functions of α and β. The actual values of all of these derivatives are assumed to be the numbers corresponding to the trim angle of attack and the trim sideslip angle. The other model parameters and constants used for the flight control design do not require the use of lookup tables. They are given in Table 2. T_m represents the maximum military thrust; $\delta_{e_{\max}}$, $\delta_{a_{\max}}$, and $\delta_{r_{\max}}$ refer to the maximum allowable deflections of the elevator, aileron, and rudder, respectively. The other symbols are according to Ref. [39]. The kinetic slow state is $x = v_A$, the kinematic slow state vector is $\xi = [\phi \quad \theta \quad \psi]^T$, the vector of fast states is $z = [p \quad q \quad r]^T$, the slow actuator is $\delta_s = \delta_t$, and the vector of fast actuators is $\delta_f = [\delta_e \quad \delta_a \quad \delta_r]^T$. The velocity dynamics can be written as

$$
\dot{x} = f_{xx}(x,\xi,\alpha,\beta) + F_{xz}(x,\alpha,\beta)z + G_{x_{\delta_s}}(\alpha,\beta)\delta_s + G_{x_{\delta_f}}(x,\alpha,\beta)\Lambda_{x_{\delta_f}}\delta_f \tag{A4}
$$

where

$$
\begin{aligned}
f_{xx}(.) &:= g(-\cos\alpha\cos\beta\sin\theta + \sin\beta\cos\theta\sin\phi \\
&\quad + \sin\alpha\cos\beta\cos\theta\cos\phi \\
&\quad + \frac{\bar{q}S}{m}[(C_{x_0} + C_{x_\alpha}\alpha)\cos\alpha\cos\beta + C_{y_\beta}\beta\sin\beta \\
&\quad + C_z(\alpha,\beta)\sin\alpha\cos\beta] \\
F_{xz}(.) &:= \begin{bmatrix} \frac{1}{m}C_{y_p}\frac{b}{2v_A}\bar{q}S\sin\beta \\ \frac{1}{m}C_{x_q}\frac{\bar{c}}{2v_A}\bar{q}S\cos\alpha\sin\beta + \frac{1}{m}C_{z_q}\frac{\bar{c}}{2v_A}\bar{q}S\sin\alpha\cos\beta \\ \frac{1}{m}C_{y_r}\frac{b}{2v_A}\bar{q}S\sin\beta \end{bmatrix}^T \\
G_{x\delta_s}(.) &:= \frac{T_m}{m}\cos\alpha\cos\beta \\
G_{x\delta_f} &:= \frac{\bar{q}S}{m}\begin{bmatrix} \cos\alpha\cos\beta \\ \sin\beta \\ \sin\alpha\cos\beta \end{bmatrix} \\
\Lambda_{x\delta_f} &:= \begin{bmatrix} C_{x_{\delta_e}} & 0 & 0 \\ 0 & C_{y_{\delta_a}} & C_{y_{\delta_r}} \\ C_{z_{\delta_e}} & 0 & 0 \end{bmatrix}
\end{aligned} \tag{A5}
$$

It is to be noted that the arguments of $f_{xx}(.)$, $F_{xz}(.)$, $G_{x\delta_s}(.)$, and $G_{x\delta_f}(.)$ contain the angle of attack α and the sideslip angle β in addition to the slow states x and ξ. For the current flight control problem, α and β are treated as known from measurement. They are not considered separately for tracking.

The Euler angles evolve according to

$$
\begin{bmatrix} \dot{\phi} \\ \dot{\theta} \\ \dot{\psi} \end{bmatrix} = \begin{bmatrix} 1 & \sin\phi\tan\theta & \cos\phi\tan\theta \\ 0 & \cos\phi & -\sin\phi \\ 0 & \frac{\sin\phi}{\cos\theta} & \frac{\cos\phi}{\cos\theta} \end{bmatrix}\begin{bmatrix} p \\ q \\ r \end{bmatrix} \tag{A6}
$$

The evolution of the Euler angles is already in the form $\dot{\xi} = F_{\xi z}(\xi)z$, where

Table 2 Some of the parameters for the generic F-16A

Parameter	Value
m	636.94 slug
g	32.17 ft/s^2
b	30 ft
S	300 ft^2
$\bar{c}$	11.32 ft
I_{xx}	9496 slug $\cdot$ ft^2
I_{yy}	55,814 slug $\cdot$ ft^2
I_{zz}	63,100 slug $\cdot$ ft^2
I_{xz}	982 slug $\cdot$ ft^2
x_{cg_r}	$0.35\bar{c}$
T_m	17,800 lbf
$\delta_{e_{\max}}$	± 25 deg
$\delta_{a_{\max}}$	± 20 deg
$\delta_{r_{\max}}$	± 30 deg
x_{cg}	$0.30\bar{c}$
C_{y_β}	-0.02/ deg
$C_{y_{\delta_a}}$	1.05×10^{-3}/deg
$C_{y_{\delta_r}}$	2.87×10^{-3}/deg
$C_{z_{\delta_e}}$	-7.6×10^{-3}/deg

$$F_{\xi z} \coloneqq \begin{bmatrix} 1 & \sin\phi\tan\theta & \cos\phi\tan\theta \\ 0 & \cos\phi & -\sin\phi \\ 0 & \frac{\sin\phi}{\cos\theta} & \frac{\cos\phi}{\cos\theta} \end{bmatrix} \tag{A7}$$

Starting from the following formulation of the evolution of the body-axis angular rates,

$$\begin{bmatrix} \dot{p} \\ \dot{q} \\ \dot{r} \end{bmatrix} = \mathcal{I}^{-1} \begin{bmatrix} 0 & 0 & I_{xz} & I_{yy}-I_{zz} & 0 \\ -I_{xz} & I_{xz} & 0 & 0 & I_{zz}-I_{xx} \\ 0 & 0 & I_{xx}-I_{yy} & -I_{xz} & 0 \end{bmatrix} [f_1(.)] + \mathcal{I}^{-1} \begin{bmatrix} L_A \\ M_A \\ N_A \end{bmatrix} \tag{A8}$$

with $[f_1(.)] \coloneqq [p^2 \quad r^2 \quad pq \quad qr \quad rp]^T$;

$$\mathcal{I} \coloneqq \begin{bmatrix} I_{xx} & 0 & -I_{xz} \\ 0 & I_{yy} & 0 \\ -I_{xz} & 0 & I_{zz} \end{bmatrix}$$

and introducing the timescale separation parameter ε artificially, Ref. [33] derives the final form:

$$\begin{aligned} \varepsilon \begin{bmatrix} \dot{p} \\ \dot{q} \\ \dot{r} \end{bmatrix} &= \begin{bmatrix} B_{11} & B_{12} & B_{13} & B_{14} & B_{15} \\ B_{21} & B_{22} & B_{23} & B_{24} & B_{25} \\ B_{31} & B_{32} & B_{33} & B_{34} & B_{35} \end{bmatrix} [f_1(.)] \\ &+ \begin{bmatrix} S_{11} & S_{12} & S_{13} \\ S_{21} & S_{22} & S_{23} \\ S_{31} & S_{32} & S_{33} \end{bmatrix} \begin{bmatrix} f_{21}(x,z,\alpha,\beta) \\ f_{22}(x,z,\alpha,\beta) \\ f_{23}(x,z,\alpha,\beta) \end{bmatrix} \\ &+ \begin{bmatrix} L_{11} & L_{12} & L_{13} \\ L_{21} & L_{22} & L_{23} \\ L_{31} & L_{32} & L_{33} \end{bmatrix} \bar{q}S \begin{bmatrix} \delta_e \\ \delta_a \\ \delta_r \end{bmatrix} \end{aligned} \tag{A9}$$

where $[S_{ij}]_{3\times 3} \coloneqq \mathcal{I}^{-1}$,

$$[B_{ij}]_{3\times 5} \coloneqq \mathcal{I}^{-1} \begin{bmatrix} 0 & 0 & I_{xz} & I_{yy}-I_{zz} & 0 \\ -I_{xz} & I_{xz} & 0 & 0 & I_{zz}-I_{xx} \\ 0 & 0 & I_{xx}-I_{yy} & -I_{xz} & 0 \end{bmatrix}$$

and

$$\begin{bmatrix} f_{21}(.) \\ f_{22}(.) \\ f_{23}(.) \end{bmatrix} \coloneqq \begin{bmatrix} \left(C_l(\alpha,\beta) + C_{l_p}\frac{pb}{2v_A} + C_{l_r}\frac{pb}{2v_A}\right)\bar{q}Sb \\ \left(C_{m_0} + C_{m_\alpha}\alpha + C_{m_q}\frac{q\bar{c}}{2v_A} + \frac{x_{\mathrm{cg}_r}-x_{\mathrm{cg}}}{\bar{c}}\left(C_z(\alpha,\beta) + C_{z_q}\frac{q\bar{c}}{2v_A}\right)\right)\bar{q}S\bar{c} \\ \left(C_n(\alpha,\beta) + C_{n_p}\frac{pb}{2v_A} + \frac{x_{\mathrm{cg}_r}-x_{\mathrm{cg}}}{b}\left(C_{y_\beta}\beta + C_{y_p}\frac{pb}{2v_A} + C_{y_r}\frac{rb}{2v_A}\right)\right)\bar{q}Sb \end{bmatrix} \tag{A10}$$

$$[L_{ij}]_{3\times 3} \coloneqq \mathcal{I}^{-1} \begin{bmatrix} 0 & C_{l_{\delta_a}} b & C_{l_{\delta_r}} b \\ \left(C_{m_{\delta_e}} + \frac{x_{\mathrm{cg}_r}-x_{\mathrm{cg}}}{\bar{c}} C_{z_{\delta_e}}\right)\bar{c} & 0 & 0 \\ 0 & \left(C_{n_{\delta_a}} + \frac{x_{\mathrm{cg}_r}-x_{\mathrm{cg}}}{b} C_{y_{\delta_a}}\right)b & \left(C_{n_{\delta_r}} + \frac{x_{\mathrm{cg}_r}-x_{\mathrm{cg}}}{b} C_{y_{\delta_r}}\right)b \end{bmatrix} \tag{A11}$$

This is equivalent to

$$\varepsilon \dot{z} = B_z^1 f_z^1 + B_z^2 f_z^2 + \Lambda_{z\delta_f} G_{z\delta_f} \delta_f \tag{A12}$$

where $B_z^1 \coloneqq [B_{ij}]_{3\times 5}$, $B_z^2 \coloneqq [S_{ij}]_{3\times 3}$, $f_z^1 \coloneqq [p^2 \quad r^2 \quad pq \quad qr \quad rp]^T$, $f_z^2 \coloneqq [f_{21}(.) \quad f_{22}(.) \quad f_{23}(.)]^T$, $\Lambda_{z\delta_f} \coloneqq [L_{ij}]_{3\times 3}$, and $G_{z\delta_f} \coloneqq \bar{q}S$. The perturbation parameters σ and ρ are introduced artificially in the actuator dynamics. The engine, elevator, aileron, and rudder are first-order actuators with time constants T_{eng}, T_{el}, T_{ail}, and T_{rud}, respectively. The engine time constant is uncertain. As a result, the functions, matrices, and parameters representing the actuator dynamics are $B_{\delta_s} \coloneqq -(1/T_{\mathrm{eng}})$, $f_{\delta_s} \coloneqq \delta_s$, $\Lambda_{\delta_s u_s} \coloneqq (1/T_{\mathrm{eng}})$, $G_{\delta_s u_s} \coloneqq 1$,

$$f_{\delta_f} \coloneqq \begin{bmatrix} -\frac{1}{T_{\mathrm{el}}}\delta_e & -\frac{1}{T_{\mathrm{ail}}}\delta_a & -\frac{1}{T_{\mathrm{rud}}}\delta_r \end{bmatrix}^T$$

and

$$G_{\delta_f u_f} \coloneqq \mathrm{diag}\left[\frac{1}{T_{\mathrm{el}}}, \frac{1}{T_{\mathrm{ail}}}, \frac{1}{T_{\mathrm{rud}}}\right]$$

No uncertain parameter is associated with the fast actuator dynamics for the aircraft simulation.

Appendix B: Proof of Theorem 1: Ultimate Boundedness of Errors

Proof: Considering the difference between the full-order and the reduced-order dynamics and simplifying, the time derivative of the composite Lyapunov function becomes

$$
\begin{aligned}
\dot{V}_c = {} & -\alpha_1(e_x^T K_x e_x + e_\xi^T K_\xi e_\xi) - \frac{\alpha_2}{\sigma} e_{\delta_s}^T K_{\delta_s} e_{\delta_s} - \frac{\alpha_3}{\varepsilon} e_z^T K_z e_z \\
& - \frac{\alpha_4}{\rho} e_{\delta_f}^T K_{\delta_f} e_{\delta_f} + \alpha_1 e_x^T [B_{xz} F_{xz} e_z + \gamma_x \\
& + \Lambda_{x\delta_s} G_{x\delta_s} e_{\delta_s} + \Lambda_{x\delta_f} G_{x\delta_f} (e_{\delta_f} + \delta_f^0 - \delta_f^0|_{z^0})] + \alpha_1 e_\xi^T F_{\xi z} e_z \\
& + \frac{\alpha_3}{\varepsilon} e_z^T (\gamma_z + \Lambda_{z\delta_f} G_{z\delta_f} e_{\delta_f}) - \alpha_2 e_{\delta_s}^T \dot{\delta}_s^0 - \alpha_3 e_z^T \dot{z}^0 - \alpha_4 e_{\delta_f}^T \dot{\delta}_f^0 \\
& + \sum_i \sum_j \tilde{b}_{xx_{ij}} \left(\alpha_1 e_{x_i} f_{xx_j} - \alpha_5 \dot{\hat{b}}_{xx_{ij}} \right) \\
& + \sum_i \sum_j \tilde{b}_{xz_{ij}} \left(\alpha_1 (e_{x_i} (F_{xz} z^0)_j - \alpha_6 \dot{\hat{b}}_{xz_{ij}} \right) \\
& + \sum_i \sum_j \tilde{\lambda}_{x\delta_{sij}} \left(\alpha_1 (e_{x_i} (G_{x\delta_s} \delta_s^0)_j - \alpha_7 \dot{\hat{\lambda}}_{x\delta_{sij}} \right) \\
& + \sum_i \sum_j \tilde{\lambda}_{x\delta_{fij}} \left(\alpha_1 (e_{x_i} (G_{x\delta_f} \delta_f^0|_{z^0})_j - \alpha_8 \dot{\hat{\lambda}}_{x\delta_{fij}} \right) \\
& + \frac{1}{\sigma} \sum_i \sum_j \tilde{b}_{\delta_{sij}} \left(\alpha_2 e_{\delta_{si}} f_{\delta_{sj}} - \alpha_9 \dot{\hat{b}}_{\delta_{sij}} \right) \\
& + \frac{1}{\sigma} \sum_i \sum_j \tilde{\lambda}_{\delta_s u_{sij}} \left(\alpha_2 e_{\delta_{si}} (G_{\delta_s u_s} u_s)_j - \alpha_{10} \dot{\hat{\lambda}}_{\delta_s u_{sij}} \right) \\
& + \frac{1}{\varepsilon} \sum_k \sum_i \sum_j \tilde{b}_{z_{ij}}^k \left(\alpha_3 e_{z_i} f_{z_j}^k - \alpha_{11k} \dot{\hat{b}}_{z_{ij}}^{k'} \right) \\
& + \frac{1}{\varepsilon} \sum_i \sum_j \tilde{\lambda}_{z\delta_{fij}} \left(\alpha_3 e_{z_i} (G_{z_{\delta_f}} \delta_f^0)_j - \alpha_{12} \dot{\hat{\lambda}}'_{z\delta_{fij}} \right) \\
& + \frac{1}{\rho} \sum_i \sum_j \tilde{b}_{\delta_{fij}} \left(\alpha_4 e_{\delta_{fi}} f_{\delta_{fj}} - \alpha_{13} \dot{\hat{b}}_{\delta_{fij}} \right) \\
& + \frac{1}{\rho} \sum_i \sum_j \tilde{\lambda}_{\delta_f u_{fij}} \left(\alpha_4 e_{\delta_{fi}} (G_{\delta_f u_f} u_f)_j - \alpha_{14} \dot{\hat{\lambda}}_{\delta_f u_{fij}} \right)
\end{aligned} \tag{B1}
$$

Selecting parameter update laws according to Eqs. (29–32), the time derivative [Eq. (B1)] becomes

$$
\begin{aligned}
\dot{V}_c = {} & -\alpha_1(e_x^T K_x e_x + e_\xi^T K_\xi e_\xi) - \frac{\alpha_2}{\sigma} e_{\delta_s}^T K_{\delta_s} e_{\delta_s} - \frac{\alpha_3}{\varepsilon} e_z^T K_z e_z \\
& - \frac{\alpha_4}{\rho} e_{\delta_f}^T K_{\delta_f} e_{\delta_f} + \alpha_1 e_x^T \left[B_{xz} F_{xz} e_z + \gamma_x \right. \\
& \left. + \Lambda_{x\delta_s} G_{x\delta_s} e_{\delta_s} + \Lambda_{x\delta_f} G_{x\delta_f} \left(e_{\delta_f} + \delta_f^0 - \delta_f^0|_{z^0} \right) \right] + \alpha_1 e_\xi^T F_{\xi z} e_z \\
& + \frac{\alpha_3}{\varepsilon} e_z^T (\gamma_z + \Lambda_{z\delta_f} G_{z\delta_f} e_{\delta_f}) - \alpha_2 e_{\delta_s}^T \dot{\delta}_s^0 - \alpha_3 e_z^T \dot{z}^0 - \alpha_4 e_{\delta_f}^T \dot{\delta}_f^0 \\
& + \theta_1 \sum_i \sum_j \tilde{b}_{xx_{ij}} \left(\hat{b}_{xx_{ij}} - b_{xx_{ij}}^0 \right) \\
& + \theta_2 \sum_i \sum_j \tilde{b}_{xz_{ij}} \left(\hat{b}_{xz_{ij}} - b_{xz_{ij}}^0 \right) + \theta_3 \sum_i \sum_j \tilde{\lambda}_{x\delta_{sij}} \left(\hat{\lambda}_{x\delta_{sij}} - \lambda_{x\delta_{sij}}^0 \right) \\
& + \theta_4 \sum_i \sum_j \tilde{\lambda}_{x\delta_{fij}} \left(\hat{\lambda}_{x\delta_{fij}} - \lambda_{x\delta_{fij}}^0 \right) \\
& + \frac{\theta_5}{\sigma} \sum_i \sum_j \tilde{b}_{\delta_{sij}} \left(\hat{b}_{\delta_{sij}} - b_{\delta_{sij}}^0 \right) + \frac{\theta_6}{\sigma} \sum_i \sum_j \tilde{\lambda}_{\delta_s u_{sij}} \left(\hat{\lambda}_{\delta_s u_{sij}} - \lambda_{\delta_s u_{sij}}^0 \right) \\
& + \frac{\theta_7}{\varepsilon} \sum_k \sum_i \sum_j \tilde{b}_{z_{ij}}^k \left(\hat{b}_{z_{ij}}^k - b_{z_{ij}}^{k^0} \right) \\
& + \frac{\theta_8}{\varepsilon} \sum_i \sum_j \tilde{\lambda}_{z\delta_{fij}} \left(\hat{\lambda}_{z\delta_{fij}} - \lambda_{z\delta_{fij}}^0 \right) + \frac{\theta_9}{\rho} \sum_i \sum_j \tilde{b}_{\delta_{fij}} \left(\hat{b}_{\delta_{fij}} - b_{\delta_{fij}}^0 \right) \\
& + \frac{\theta_{10}}{\rho} \sum_i \sum_j \tilde{\lambda}_{\delta_f u_{fij}} \left(\hat{\lambda}_{\delta_f u_{fij}} - \lambda_{\delta_f u_{fij}}^0 \right)
\end{aligned} \tag{B2}
$$

Equation (B2) has some terms to be upper bounded. For any constant but unknown parameter p bounded as $\underline{p} \le p \le \bar{p}$, the expression

$$
\begin{aligned}
\tilde{p}(\hat{p} - p^0) &= \tilde{p}(p - \tilde{p} - p^0) = \tilde{p}(p - p^0) - \tilde{p}^2 \\
&\le \frac{1}{2}[\tilde{p}^2 + (p - p^0)^2] - \tilde{p}^2 \le \frac{1}{2} \max_{\underline{p} \le p \le \bar{p}} (p - p^0)^2 - \frac{1}{2}\tilde{p}^2 \\
&= \frac{1}{2} p^+ - \frac{1}{2}\tilde{p}^2
\end{aligned}
$$

where

$$
p^+ = \max_{\underline{p} \le p \le \bar{p}} (p - p^0)^2
$$

Extending this result to all the parameters, Eq. (B2) can be upper bounded as

$$
\begin{aligned}
\dot{V}_c \le {} & -\alpha_1(e_x^T K_x e_x + e_\xi^T K_\xi e_\xi) - \frac{\alpha_2}{\sigma} e_{\delta_s}^T K_{\delta_s} e_{\delta_s} - \frac{\alpha_3}{\varepsilon} e_z^T K_z e_z \\
& - \frac{\alpha_4}{\rho} e_{\delta_f}^T K_{\delta_f} e_{\delta_f} + \alpha_1 e_x^T [B_{xz} F_{xz} e_z + \gamma_x + \Lambda_{x\delta_s} G_{x\delta_s} e_{\delta_s} \\
& + \Lambda_{x\delta_f} G_{x\delta_f} (e_{\delta_f} + \delta_f^0 - \delta_f^0|_{z^0})] + \alpha_1 e_\xi^T F_{\xi z} e_z \\
& + \frac{\alpha_3}{\varepsilon} e_z^T (\gamma_z + \Lambda_{z\delta_f} G_{z\delta_f} e_{\delta_f}) - \alpha_2 e_{\delta_s}^T \dot{\delta}_s^0 - \alpha_3 e_z^T \dot{z}^0 - \alpha_4 e_{\delta_f}^T \dot{\delta}_f^0 \\
& - \frac{\theta_1}{2} \sum_i \sum_j \tilde{b}_{xx_{ij}}^2 - \frac{\theta_2}{2} \sum_i \sum_j \tilde{b}_{xz_{ij}}^2 - \frac{\theta_3}{2} \sum_i \sum_j \tilde{\lambda}_{x\delta_{sij}}^2 \\
& - \frac{\theta_4}{2} \sum_i \sum_j \tilde{\lambda}_{x\delta_{fij}}^2 - \frac{\theta_5}{2\sigma} \sum_i \sum_j \tilde{b}_{\delta_{sij}}^2 - \frac{\theta_6}{2\sigma} \sum_i \sum_j \tilde{\lambda}_{\delta_s u_{\mathrm{sij}}}^2 \\
& - \frac{\theta_7}{2\varepsilon} \sum_k \sum_i \sum_j \tilde{b}_{z_{ij}}^{k^2} - \frac{\theta_8}{2\varepsilon} \sum_i \sum_j \tilde{\lambda}_{z\delta_{fij}}^2 - \frac{\theta_9}{2\rho} \sum_i \sum_j \tilde{b}_{\delta_{fij}}^2 \\
& - \frac{\theta_{10}}{2\rho} \sum_i \sum_j \tilde{\lambda}_{\delta_f u_{fij}}^2 + \mu_0
\end{aligned} \tag{B3}
$$

where

$$
\begin{aligned}
\mu_0 \coloneqq {} & \frac{\theta_1}{2} \sum_i \sum_j b_{xx_{ij}}^+ + \frac{\theta_2}{2} \sum_i \sum_j b_{xz_{ij}}^+ + \frac{\theta_3}{2} \sum_i \sum_j \lambda_{x\delta_{sij}}^+ \\
& + \frac{\theta_4}{2} \sum_i \sum_j \lambda_{x\delta_{fij}}^+ + \frac{\theta_5}{2\sigma} \sum_i \sum_j b_{\delta_{sij}}^+ + \frac{\theta_6}{2\sigma} \sum_i \sum_j \lambda_{\delta_s u_{sij}}^+ \\
& + \frac{\theta_7}{2\varepsilon} \sum_k \sum_i \sum_j b_{z_{ij}}^{k^+} + \frac{\theta_8}{2\varepsilon} \sum_i \sum_j \lambda_{z\delta_{fij}}^+ + \frac{\theta_9}{2\rho} \sum_i \sum_j b_{\delta_{fij}}^+ \\
& + \frac{\theta_{10}}{2\rho} \sum_i \sum_j \lambda_{\delta_f u_{fij}}^+
\end{aligned} \tag{B4}
$$

Equation (B3) has some terms that involve the equilibrium manifolds and their time derivatives. Given the mathematical expressions of the manifolds chosen during controller design, it is difficult to use the exact expressions of either the manifolds themselves or their time derivatives. To find upper bounds of these terms, the extreme value theorem is used in a manner similar to the approach of Swaroop et al. [40,41]. Let N_1 denote the combined dimension of the states and the unknown parameters. Consider a compact set $Q_1 \in \mathbb{R}^{N_1}$ characterized by the composite Lyapunov function in Eq. (27) and upper bounded by $\bar{V}$; i.e., $V_c \le \bar{V}$ for some $\bar{V} > 0$. Let N_2 denote the combined dimension of the references and their time derivatives of first and second orders. Consider a compact set $Q_2 \in \mathbb{R}^{N_2}$, characterized by

$$
\|x_r\|_2^2 + \|\dot{x}_r\|_2^2 + \|\ddot{x}_r\|_2^2 + \|\xi_r\|_2^2 + \|\dot{\xi}_r\|_2^2 + \|\ddot{\xi}_r\|_2^2 \le R^2
$$

for some $R > 0$. Then, $Q \coloneqq Q_1 \times Q_2$ is a compact set in $\mathbb{R}^{N_1+N_2}$, and all the elements of the vectors z^0, $\delta_f^0 - \delta_f^0|_{z^0}$, $\dot{\delta}_s^0$, $\dot{z}^0$, and $\dot{\delta}_f^0$ are continuous functions in the compact set Q. Therefore, each element of these vectors has a maximum; consequently, there exist constants

M_1, M_2, M_3, M_4, and M_5 such that $\|z^0\|_\infty = M_1$, $\|\delta_f^0 - \delta_f^0|_{z^0}\|_\infty = M_2$, $\|\dot{\delta}_s^0\|_\infty = M_3$, $\|\dot{z}^0\|_\infty = M_4$, and $\|\dot{\delta}_f^0\|_\infty = M_5$. Upper bounds of other cross terms involving the products of errors can be found by using the following results: 1) Cauchy–Schwarz inequality of $u^T v \le \|u\|_2\|v\|_2$, 2) property of induced norm of matrices of $\|Ax\| \le \|A\|\|x\|$, 3) induced 2-norm of a matrix that is the same as its largest singular value, 4) Young's inequality of $ab \le (1/2)(a^2 + b^2)$, and 5) introduction of artificial variables to obtain quadratic bound using Young's inequality:

$$\|v\|_2 \le \frac{1}{2}\left(\chi_i^2 + \frac{1}{\chi_i^2}\|v\|_2^2\right)$$

for any arbitrary nonzero χ_i. Using all of these results, the time derivative of the composite Lyapunov function [Eq. (B3)] reduces to the following:

$$\begin{aligned}\dot{V}_c \le & -\beta_1 e_x^T e_x - \beta_2 e_\xi^T e_\xi - \beta_3 e_{\delta_s}^T e_{\delta_s} - \beta_4 e_z^T e_z - \beta_5 e_{\delta_f}^T e_{\delta_f} - \frac{\theta_1}{2}\sum_j \tilde{b}_{xx_{ij}}^2 \\ & - \frac{\theta_2}{2}\sum_i\sum_j \tilde{b}_{xz_{ij}}^2 - \frac{\theta_3}{2}\sum_i\sum_j \tilde{\lambda}_{x\delta_{sij}}^2 - \frac{\theta_4}{2}\sum_i\sum_j \tilde{\lambda}_{x\delta_{fij}}^2 \\ & - \frac{\theta_5}{2\sigma}\sum_i\sum_j \tilde{b}_{\delta_{sij}}^2 - \frac{\theta_6}{2\sigma}\sum_i\sum_j \tilde{\lambda}_{\delta_s u_{sij}}^2 - \frac{\theta_7}{2\varepsilon}\sum_k\sum_i\sum_j \tilde{b}_{z_{ij}}^{k^2} \\ & - \frac{\theta_8}{2\varepsilon}\sum_i\sum_j \tilde{\lambda}_{z\delta_{fij}}^2 - \frac{\theta_9}{2\rho}\sum_i\sum_j \tilde{b}_{\delta_{fij}}^2 - \frac{\theta_{10}}{2\rho}\sum_i\sum_j \tilde{\lambda}_{\delta_f u_{fij}}^2 + \mu\end{aligned} \tag{B5}$$

where $\beta_i; i = 1, 2, 3, 4, 5$ are given by

$$\begin{aligned}\beta_1 &:= \frac{1}{2}\alpha_1\left(2\lambda_{\min}(K_x) - (2\kappa_1 + \kappa_2 + \kappa_3) - v_1 v_2 \right. \\ &\quad \left. - \frac{\kappa_1 R + \kappa_2 R + \kappa_3 M_1\sqrt{m}}{\chi_1^2} - v_3 v_4 - v_5 v_6 - \frac{v_5 v_6 M_2\sqrt{m}}{\chi_1^2}\right) \\ &\quad - \frac{\alpha_3\kappa_4}{2\varepsilon} := \alpha_1\lambda_{\min}(K_x) - \bar{\beta}_1 - \frac{\alpha_3 k_4}{2\varepsilon} \\ \beta_2 &:= \frac{\alpha_1}{2}(2\lambda_{\min}(K_\xi) - \kappa_2 - v_7) - \frac{\alpha_3\kappa_5}{2\varepsilon} \\ \beta_3 &:= \frac{1}{2}\left(2\frac{\alpha_2}{\sigma}\lambda_{\min}(K_{\delta_s}) - \alpha_1 v_3 v_4 - \frac{\alpha_2 M_3\sqrt{n}}{\chi_2^2}\right) := \frac{\alpha_2}{\sigma}\lambda_{\min}(K_{\delta_s}) - \bar{\beta}_3 \\ \beta_4 &:= \frac{1}{2}\frac{\alpha_3}{\varepsilon}\left(2\lambda_{\min}(K_z) - (\kappa_4 + \kappa_5 + 2\kappa_6) - \frac{\kappa_4 R + \kappa_5 R + \kappa_6 M_1\sqrt{m}}{\chi_3^2}\right. \\ &\quad \left. - v_8 v_9 - \frac{M_4\sqrt{m}}{\chi_3^2}\right) - \frac{\alpha_1}{2}(v_1 v_2 + \kappa_3 + v_7) \\ &:= \frac{\alpha_3}{\varepsilon}(\lambda_{\min}(K_z) - \beta_{41}) - \beta_{42} \\ \beta_5 &:= \frac{1}{2}\left(2\frac{\alpha_4}{\rho}\lambda_{\min}(K_{\delta_f}) - \frac{\alpha_4 M_5\sqrt{m}}{\chi_4^2} - \alpha_1 v_5 v_6 - \frac{\alpha_3}{\varepsilon}v_8 v_9\right) \\ &:= \frac{\alpha_4}{\rho}\lambda_{\min}(K_{\delta_f}) - \bar{\beta}_5 - \frac{\alpha_3 v_8 v_9}{\varepsilon}\end{aligned} \tag{B6}$$

where $\lambda_{\min}(A)$ is the minimum eigenvalue of a matrix A, and the constants $\bar{\beta}_1, \bar{\beta}_3, \bar{\beta}_5, \beta_{41}$, and β_{42} contain the terms involving neither the gains $K_x, K_\xi, K_z, K_{\delta_s}$, and K_{δ_f} nor the perturbation parameters σ, ε, and ρ. The factor μ is given by

$$\begin{aligned}\mu := \mu_0 + \frac{1}{2}\Big[&\alpha_1\left(\kappa_1 R + \kappa_2 R + \kappa_3 M_1\sqrt{m}\right)\chi_1^2 + \alpha_1 v_5 v_6 M_2\sqrt{m}\chi_1^2 \\ &+ \frac{\alpha_3}{\varepsilon}\left(\kappa_4 R + \kappa_5 R + \kappa_6 M_1\sqrt{m}\right)\chi_3^2 \\ &+ \alpha_2 M_3\sqrt{n}\chi_2^2 + \alpha_3 M_4\sqrt{m}\chi_3^2 + \alpha_4 M_5\sqrt{m}\chi_4^2\Big]\end{aligned} \tag{B7}$$

with μ_0 given by Eq. (B4). Note that μ can be written in the form

$$\mu = \mu_1 + \frac{\mu_2}{\sigma} + \frac{\mu_3}{\varepsilon} + \frac{\mu_4}{\rho} \tag{B8}$$

where $\mu_i, i = 1, 2, 3, 4$ are constants. Furthermore, define the following:

$$\begin{aligned}\eta &:= \min\left\{\beta_1, \beta_2, \beta_3, \beta_4, \beta_5, \frac{\theta_1}{2}, \frac{\theta_2}{2}, \frac{\theta_3}{2}, \frac{\theta_4}{2}, \frac{\theta_5}{2\sigma}, \frac{\theta_6}{2\sigma}, \frac{\theta_7}{2\varepsilon}, \frac{\theta_8}{2\varepsilon}, \frac{\theta_9}{2\rho}, \frac{\theta_{10}}{2\rho}\right\} \\ \bar{\eta} &:= \frac{1}{2}\max\{\alpha_1, \ldots, \alpha_{10}, \alpha_{11k}, \alpha_{12}, \ldots, \alpha_{14}\}\end{aligned} \tag{B9}$$

In addition, consider e to be the vector formed by stacking up in one column all the errors: tracking errors for the slow states, deviation from equilibrium manifolds of fast states and actuators, and all parameter estimation errors. Inequality (B5) can be expressed as

$$\begin{aligned}\dot{V}_c &\le -\eta\|e\|_2^2 + \mu \\ &\le -\frac{\eta}{\bar{\eta}}V_c + \mu\end{aligned} \tag{B10}$$

Inequality (B10) shows that $\dot{V}_c$ is negative outside the compact set

$$\|e\|_2 > \sqrt{\frac{\mu}{\eta}}$$

Therefore, the errors will be ultimately bounded within

$$0 \le \|e\|_2 \le \sqrt{\frac{\mu}{\eta}}$$

Suppose that it is desired to keep the error vector e ultimately bounded within a ball of radius θ_r; i.e., $\dot{V}_c < 0$ on the boundary of the ball represented by $\|e\|_2 = \theta_r$. This is possible if $-\eta\theta_r^2 + \mu < 0$; i.e., if

$$\eta > \frac{\mu}{\theta_r^2} \tag{B11}$$

This is equivalent to saying that every element in the set

$$\mathcal{A} := \left\{\beta_1, \beta_2, \beta_3, \beta_4, \beta_5, \frac{\theta_1}{2}, \frac{\theta_2}{2}, \frac{\theta_3}{2}, \frac{\theta_4}{2}, \frac{\theta_5}{2\sigma}, \frac{\theta_6}{2\sigma}, \frac{\theta_7}{2\varepsilon}, \frac{\theta_8}{2\varepsilon}, \frac{\theta_9}{2\rho}, \frac{\theta_{10}}{2\rho}\right\}$$

is greater than (μ/θ_r^2). Therefore, if the gains and other design variables are chosen such that every element in the set $\mathcal{A}$ exceeds (μ/θ_r^2) for some σ, ε, and $\rho > 0$, then there exist bounds $\sigma_{**}, \sigma^{**}, \varepsilon_{**}, \varepsilon^{**}, \rho_{**}$, and ρ^{**} such that the ultimate boundedness of errors is guaranteed for $\sigma_{**} \le \sigma \le \sigma^{**}$, $\varepsilon_{**} \le \varepsilon \le \varepsilon^{**}$, and $\rho_{**} \le \rho \le \rho^{**}$. This completes the proof. □

The inclusion of parametric uncertainties in actuator dynamics leads to a set of coupled inequalities [Eq. (B11)]. The solutions to these inequalities are the bounds of timescale separation parameters for the ultimate boundedness of errors. If the actuators are assumed free of uncertainty, these inequalities can be simplified to obtain closed-form bounds of timescale separation [33].

Acknowledgment

The authors would like to acknowledge Venkata Sravan Akkinapalli for his insightful discussion on the geometric singular perturbation and nonlinear dynamic inversion controllers.

References

[1] Khalil, H. K., and Chen, F.-C., "Two-Time-Scale Longitudinal Control of Airplanes Using Singular Perturbation," *Journal of Guidance,*

Control, and Dynamics, Vol. 13, No. 6, 1990, pp. 952–960. https://doi.org/10.2514/3.20566

[2] Shahravi, M., and Azimi, M., "Attitude and Vibration Control of Flexible Spacecraft Using Singular Perturbation Approach," *ISRN Aerospace Engineering*, Vol. 2014, 2014, Paper 163870. https://doi.org/10.1155/2014/163870

[3] Tavasoli, A., Eghtesad, M., and Jafarian, H., "Two-Time Scale Control and Observer Design for Trajectory Tracking of Two Cooperating Robot Manipulators Moving a Flexible Beam," *Robotics and Autonomous Systems*, Vol. 57, No. 2, 2009, pp. 212–221. https://doi.org/10.1016/j.robot.2008.04.003

[4] Sauer, P. W., "Time-Scale Features and Their Applications in Electric Power Systems Dynamic Modeling and Analysis," *Proceedings of the American Control Conference*, IEEE, New York, 2011, pp. 4155–4159. https://doi.org/10.1109/ACC.2011.5991375

[5] Mélykúti, B., Hespanha, J. P., and Khammash, M., "Equilibrium Distributions of Simple Biochemical Reaction Systems for Time Scale Separation in Stochastic Reaction Networks," *Journal of the Royal Society Interface*, Vol. 11, No. 97, 2014. https://doi.org/10.1098/rsif.2014.0054

[6] Shimjith, S. R., Tiwari, A. P., and Bandyopadhyay, B., *Modeling and Control of a Large Nuclear Reactor: A Three-Time-Scale Approach*, Lecture Notes in Control and Information Sciences, Vol. 431, Springer, Berlin, 2013, pp. 101–114. https://doi.org/10.1007/978-3-642-30589-4

[7] Soner, H. M., "Singular Perturbations in Manufacturing," *SIAM Journal on Control and Optimization*, Vol. 31, No. 1, 1993, pp. 132–146. https://doi.org/10.1137/0331010

[8] Fenichel, N., "Geometric Singular Perturbation Theory for Ordinary Differential Equations," *Journal of Differential Equations*, Vol. 31, No. 1, 1979, pp. 53–98. https://doi.org/10.1016/0022-0396(79)90152-9

[9] Kokotovic, P., Khalil, H. K., and O'Reilly, J., *Singular Perturbation Methods in Control: Analysis and Design*, SIAM, Philadelphia, PA, 1986. https://doi.org/10.1137/1.9781611971118

[10] Narang-Siddarth, A., and Valasek, J., *Nonlinear Time Scale Systems in Standard and Nonstandard Forms: Analysis and Control*, SIAM, Philadelphia, PA, 2014, pp. 1–108. https://doi.org/10.1137/1.9781611973341

[11] Kuo, F. Y., and Sloan, I. H., "Lifting the Curse of Dimensionality," *Notices of the AMS*, Vol. 52, No. 11, 2005, pp. 1320–1328.

[12] Khalil, H. K., *Nonlinear Systems*, 3rd ed., Prentice–Hall, Upper Saddle River, NJ, 2002, pp. 423–468.

[13] Tikhonov, A. N., "Systems of Differential Equations Containing Small Parameters Multiplying Some of the Derivatives," *Mathematic Sbovenic*, Vol. 31, No. 73, 1952, pp. 575–586.

[14] Vasileva, A. B., "Asymptotic Behavior of Solutions to Certain Problems Involving Nonlinear Ordinary Differential Equations Containing a Small Parameter Multiplying the Highest Derivatives," *Russian Mathematical Surveys*, Vol. 18, No. 3, 1963, pp. 13–84. https://doi.org/10.1070/RM1963v018n03ABEH001137

[15] Kokotovic, P. V., and Sannuti, P., "Singular Perturbation Method for Reducing Model Order in Optimal Control Design," *IEEE Transactions on Automatic Control*, Vol. 13, No. 4, 1968, pp. 377–384. https://doi.org/10.1109/TAC.1968.1098927

[16] Sannuti, P., and Kokotovic, P. V., "Near Optimum Design of Linear Systems by Singular Perturbation Method," *IEEE Transactions on Automatic Control*, Vol. 14, No. 1, 1969, pp. 15–22. https://doi.org/10.1109/TAC.1969.1099113

[17] Kokotovic, P. V., O'Malley, R. E., and Sannuti, P. V., "Singular Perturbation Methods and Order Reduction in Control Theory—An Overview," *Automatica*, Vol. 12, No. 2, 1976, pp. 123–132. https://doi.org/10.1016/0005-1098(76)90076-5

[18] Naidu, D. S., and Calise, A. J., "Singular Perturbations and Time Scales in Guidance and Control of Aerospace Systems: A Survey," *Journal of Guidance, Control, and Dynamics*, Vol. 24, No. 6, 2001, pp. 1057–1078. https://doi.org/10.2514/2.4830

[19] Naidu, D. S., "Singular Perturbations and Time-Scales in Control Theory and Applications," *Dynamics of Continuous, Discrete and Impulsive Systems, Series B: Applications and Algorithms*, Vol. 9, No. 2, 1976, pp. 233–278.

[20] O'Malley, R. E., *Singular Perturbation Methods for Ordinary Differential Equations*, Springer–Verlag, New York, 1991.

[21] O'Malley, R. E., *Historical Developments in Singular Perturbations*, Springer, New York, 2014.

[22] Narang-Siddarth, A., and Valasek, J., "Kinetic State Tracking for a Class of Singularly Perturbed Systems," *Journal of Guidance, Control, and Dynamics*, Vol. 34, No. 3, 2011, pp. 734–749. https://doi.org/10.2514/1.52127

[23] Menon, P. K. A., Chatterji, G. B., and Cheng, V. H. L., "A Two-Time-Scale Autopilot for High Performance Aircraft," *AIAA Guidance, Navigation and Control Conference*, AIAA Paper 1991-2674, 1991. https://doi.org/10.2514/6.1991-2674

[24] Narang-Siddarth, A., and Valasek, J., "Global Tracking Control Structures for Nonlinear Singularly Perturbed Aircraft Systems," *Advances in Aerospace Guidance, Navigation and Control*, edited by F. Holzapfel and S. Theil, Springer, Berlin, 2011, pp. 235–246; also *Proceedings of the 1st CEAS Specialist Conference on Guidance, Navigation and Control, (Euro GNC 2011)*, Munich, Germany, April 2011. https://doi.org/10.1007/978-3-642-19817-5_19

[25] Saha, D., Valasek, J., Famularo, D., and Reza, M. M., "Combined Longitudinal and Lateral/Directional Maneuvers of a Generic F-16A Using Multiple-Time-Scale Control," *AIAA Guidance, Navigation and Control Conference, AIAA SciTech*, AIAA Paper 2018-1335, Jan. 2018. https://doi.org/10.2514/6.2018-1335

[26] Valasek, J., "A Study of a Modified Torsional Agility Metric Using Simulation Methods," M.S. Thesis, Dept. of Aerospace Engineering, Univ. of Kansas, Lawrence, KS, 1990.

[27] Roskam, J., *Airplane Design Part V: Component Weight Estimation*, DARcorporation, Lawrence, KS, 2003, pp. 17–22.

[28] Saha, D., Valasek, J., and Reza, M. M., "Two-Time-Scale Control of a Low-Order Nonlinear Nonstandard System with Uncertain Dynamics," *Proceedings of the American Control Conference*, IEEE, New York, June 2018, pp. 3720–3725. https://doi.org/10.23919/ACC.2018.8431384

[29] Slotine, J. E., and Li, W., *Applied Nonlinear Control*, Prentice–Hall, Upper Saddle River, NJ, 1991, pp. 122–125.

[30] Saha, D., and Valasek, J., "Nonlinear Multiple-Time-Scale Attitude Control of a Rigid Spacecraft with Uncertain Inertias," *AIAA Guidance, Navigation and Control Conference, AIAA SciTech*, AIAA Paper 2019-0932, Jan. 2019. https://doi.org/10.2514/6.2019-0932

[31] Wang, J., Holzapfel, F., and Peter, F., "Comparison of Nonlinear Dynamic Inversion and Backstepping Controls with Application to a Quadrotor," *Proceedings of the EuroGNC 2013, 2nd CEAS Specialist Conference on Guidance, Navigation and Control*, Council of European Aerospace Societies (CEAS), Brussels, Belgium, April 2013, pp. 1245–1263.

[32] Wang, J., "Novel Control Approaches to Quadrotors Inspired by Dynamic Inversion and Backstepping," Ph.D. Dissertation, Technical Univ. of Munich, Munich, Germany, 2014.

[33] Saha, D., "Full-State and Output Feedback Control of Uncertain Nonlinear Nonstandard Multiple-Time-Scale Systems," Ph.D. Dissertation, Texas A&M Univ., College Station, TX, 2018.

[34] Dong, W., and Kuhnert, K. D., "Robust Adaptive Control of Nonholonomic Mobile Robot with Parameter and Nonparameter Uncertainties," *IEEE Transactions on Robotics*, Vol. 21, No. 2, 2005, pp. 261–266. https://doi.org/10.1109/TRO.2004.837236

[35] Snell, S. A., Enns, D. F., and Garrard, W. L., "Nonlinear Inversion Flight Control for a Supermaneuverable Aircraft," *Journal of Guidance, Control, and Dynamics*, Vol. 15, No. 4, 1992, pp. 976–984. https://doi.org/10.2514/3.20932

[36] Miller, C. J., "Nonlinear Dynamic Inversion Baseline Control Law: Flight-Test Results for the Full-Scale Advanced Systems Testbed F/A-18 Airplane," *AIAA Guidance, Navigation and Control Conference, AIAA SciTech*, AIAA Paper 2011-6468, Aug. 2011. https://doi.org/10.2514/6.2011-6468

[37] Hameduddin, I., and Bajodah, A. H., "Nonlinear Generalized Dynamic Inversion for Aircraft Maneuvering Control," *International Journal of Control*, Vol. 85, No. 4, 2012, pp. 437–450. https://doi.org/10.1080/00207179.2012.656143

[38] Saha, D., and Valasek, J., "Two-Time-Scale Slow and Fast State Tracking of a Generic F-16 Using Slow and Fast Controls," *AIAA Guidance, Navigation and Control Conference, AIAA SciTech*, AIAA Paper 2017-1256, Jan. 2017. https://doi.org/10.2514/6.2017-1256

[39] Stevens, B. L., and Lewis, F. L., *Aircraft Control and Simulation*, 2nd ed., Wiley, Hoboken, NJ, 2003, pp. 116–210, 584–592.

[40] Swaroop, D., Gerdes, J. C., Yip, P. P., and Hedrick, J. K., "Dynamic Surface Control of Nonlinear Systems," *Proceedings of the American Control Conference*, Albuquerque, NM, June 1997, pp. 3028–3034. https://doi.org/10.1109/ACC.1997.612013

[41] Swaroop, D., Hedrick, J. K., Yip, P. P., and Gerdes, J. C., "Dynamic Surface Control for a Class of Nonlinear Systems," *IEEE Transactions on Automatic Control*, Vol. 45, No. 10, 2000, pp. 1893–1899. https://doi.org/10.1109/TAC.2000.880994